

Quark structure of hadrons and high energy collisions

J. Nyiri

Research Institute for Particle and Nuclear Physics
Budapest, Hungary

October 29, 2018

Contents

1	The quark structure of hadrons	4
2	Multiparticle production processes	7
2.1	General description of the approach. The spectator mechanism	7
2.2	Quark combinatorics	10
2.3	Probabilities of the production of hadron states in the central and fragmentation regions	15
2.4	Multiplicities of the secondary particles in the central and fragmentation regions	16
3	Quark combinatorics in hadronic Z^0 decays	23
3.1	Prompt production in the central region of the quark jet and the vector-pseudoscalar ratio	26
3.2	Inclusive production of mesons in the fragmentation region	34
3.3	Suppression of the strange and heavy quark productions	37
3.4	Baryon-meson ratio and the Watson-Migdal factor	44
4	Hadron - nucleus interaction	45

arXiv:hep-ph/0207155v1 12 Jul 2002

Foreword

There exists a large field for phenomenological models in which the knowledge of the structure of hadrons in terms of QCD constituents obtained from deep inelastic scatterings is related to their behaviour in soft processes. One of the simplest and oldest models is the additive quark model, with the rules of quark statistics following from it. Originally, the relations of quark combinatorics for hadron yields were based on the qualitative description of a multiparticle production process as a process of the production of non-correlated quarks and antiquarks followed by their subsequent fusion into hadrons [20],[21]. An analogy with the statistical description of multinucleon processes was used, including the fact that there are final state interactions both in multinucleon reactions and in multi-quark reactions. In the latter case it was natural to suppose [9] that $q\bar{q}$ and qqq final state interactions lead to the dominant contribution of comparatively low-mass mesons and baryons into the spectra of the produced hadrons.

The additive quark model turned out to be rather successful in describing different experimental data. The model for hadronization suggested in [20],[21] which is based on the hypothesis of soft colour neutralization is used up to now when considering hadron production in jets [36]. As a large amount of new precision measurements appear, and, on the other hand, our understanding of QCD becomes deeper, a new level of understanding of quark-gluon physics in the region of soft interactions forces us to review the relations of quark combinatorics. To do so, an especially good possibility is provided by the experimental data for hadronic Z^0 decays which allow us to check the relations of quark combinatorics for a new type of processes: quark jets in the decays $Z^0 \rightarrow q\bar{q} \rightarrow \text{hadrons}$ [32].

Introduction

All the recent conceptions of strong interactions are based on the notion of quarks [1] which appeared in the early sixties as a mathematical expression of the SU(3) symmetry properties of hadrons. Since then, it had gone through a long way of evolution. We are sure today that all the complexity of hadronic phenomena is due to the fact that hadrons are composite systems built up from a small number of "elementary" particles, quarks and gluons. Quarks as objects inside the hadrons appeared first in the "classical" models of constituent quarks ([2]-[4]). The quark model gave a comprehensive tool for classifying the hadronic states. Its success turned out to be not just descriptive, but quantitatively accurate; in many cases the consequences of the model were known before data were available, and new hadrons were found due to these predictions.

Strong evidence for the quark structure of hadrons was provided by the investigation of hard processes, such as deep inelastic scatterings of high-energy electrons, muons and neutrinos on hadrons (in practice, nucleons), $\mu^+\mu^-$ production with large effective masses in hadron collisions, e^+e^- annihilation into hadrons. Indeed, the quantitative description of these processes on the basis of the parton model required the introduction of point-like objects, the symmetry properties of which coincides with those of the constituent quarks. Also, it turned out, that in the framework of the quark model hadron-hadron collision processes at high energies could also be handled ([5]-[7]).

The problem is that while in the theory we deal with microscopic dynamics of quarks

and gluons, we want to understand the spectrum and interactions of hadrons. Quantum chromodynamics is the microscopic theory of hadrons and their interactions, the success of the QCD-based phenomenology leaves no doubt about that. It contains the free quarks supplied with the required colour degrees of freedom. Being an asymptotically free theory, i.e. a theory in which interactions at short distances (at large momentum transfers) are small, QCD gives a description of hard processes which is in accordance with the prediction of the parton model. At large distances the interaction increases, and we face the phenomenon of quark confinement.

There exist different approaches to explain it within QCD. According to Gribov ([8] and references therein), the confinement is a property of our world and it is largely determined by the existence of practically massless quarks. QCD is here formulated as a quantum field theory containing both perturbative and non-perturbative phenomena, and the confinement is based on the supercritical binding of light quarks. The theory of the supercritical confinement seems to be, at present, the only possibility to give a natural explanation for the dynamical mechanism of the interaction.

If the proposed theory proves to be successful, it means that we can go down to the small momentum scale which implies understanding and describing the physics of confinement essentially perturbatively. Still, up to now, when considering soft processes, one has to deal with all the problems connected with strong interactions. It is reasonable, therefore, to describe soft processes in a different, semi-phenomenological way, which is in agreement with the experimental data and at the same time does not contradict the theory, moreover, gives some indications to the character of the confinement. Hence, one can hope that even if the problem of the confinement is solved, the results of this semi-phenomenological description remain valid.

We review here an approach that enables us to handle soft processes¹. This is based on a hadron picture due to which the baryons (and mesons) are formed by three (or, respectively, two) constituent quarks which are separated in space, i.e. the sizes of the quarks are much less than those of the hadrons ([10],[11]). The presence of three or two discrete objects in a hadron can be reconciled with the parton picture assuming that a fast moving hadron is a system of three (or two) spatially separated clouds of partons, each containing a valence quark, a sea of quark-antiquark pairs and gluons. In the case of such a hadron, which, like a nucleus, is characterized by two different sizes, the impulse approximation can be applied for hadron collisions at high energies.

There are several experimental facts which seem to support this hadron picture. In elastic hadron-hadron scattering processes at high energies the shrinkage of the diffraction cone was observed. The parameter α'_p (the slope of the Pomeron) characterizing the shrinkage is small compared to the slope of the diffractive cone itself. This is an indication for the existence of a second, characteristic size inside the hadron (in addition to the size of the hadron itself) which could be the small radius of the constituent quark [10]. Theoretical arguments have also been expressed in favour of such a double structure of hadrons. Due to [12], the confinement region of gluonium states might be much less than that of the quarks, i.e. the "coat" of the constituent quark is consisting mainly of gluons. Another possibility to explain the existence of two sizes comes from instanton-type fluctuations in the QCD vacuum [13].

The considered hadron picture is, of course, a simplified one. Still, apart from describ-

¹A detailed description of this approach is given in [9].

ing well the soft processes at high energies, it gives a possibility to connect the results of investigations in hard processes [14],[15] with the "old" quark physics.

1 The quark structure of hadrons

The first serious success of the quasi-nuclear quark model was the description of static properties of hadrons. Hadron spectroscopy gave and continues to give results which confirm the quark structure of hadrons. Also, the calculated magnetic moments of baryons as well as the decay widths of vector mesons were in reasonably good agreement with the experimental data.

There is another field where the additive quark model is rather successful: the description of hadron collision processes at moderately high energies.

Let us remind now the well-known arguments which support the impulse approximation² in hadron collision processes at high energies. Comparing theoretical predictions with experimental data, it turned out that the processes

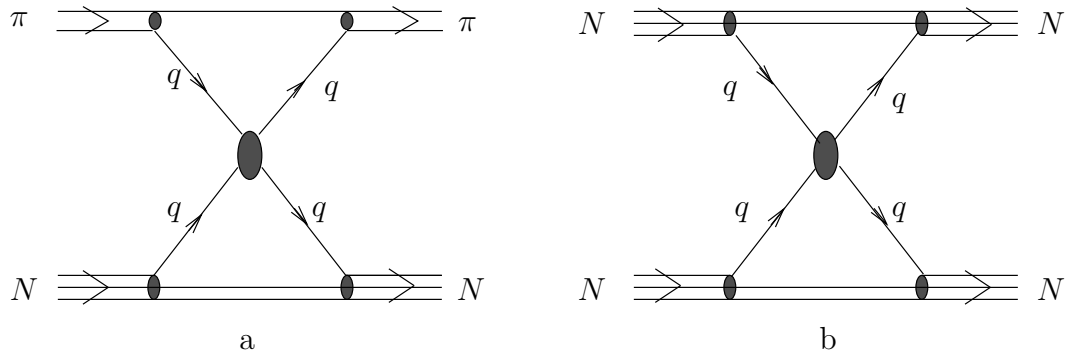


Fig.1

describe sufficiently well the ratio of the total cross sections in NN and πN scattering ([5]-[7])

$$\frac{\sigma_{tot}(NN)}{\sigma_{tot}(\pi N)} = \frac{3}{2} \quad (1)$$

as well as the decrease of the elastic pp - cross section with the increase of the momentum transfer [6]

$$\frac{d\sigma(\pi p \rightarrow \pi p)}{dt} = |a_{qq}(t)|^2 F_p^2(t) F_\pi^2(t), \quad (2)$$

²The notion of impulse approximation comes from the deep inelastic scattering of an electron on a nucleus, when the momentum transfer is much larger than the average internal momentum of the nucleons in the ground state. Under these conditions the interaction between the electron and the nucleons is so sudden, and the change of the momentum is so large that one can neglect the binding forces between the constituents during the collision. In the first approximation, the constituents behave like free particles. This is called the impulse approximation; the electron can be considered as being scattered by one of the "free" nucleons.

We can apply this analogy to the scattering process by an isolated nucleon. The rôle of the electrons is played by one of the leptons, that of the nucleus by the nucleon, and that of nucleons within the nucleus by quarks. There is, of course, an important difference: because of confinement, quarks cannot be ejected from the nucleon. This, however, is not significant from the point of view of the scattering cross section. On the other hand, the properties of the final states depend on the mechanisms that appear when the highly energetic quark attempts to leave the hadron. At this stage quark-antiquark pairs are produced which eventually materialize into new hadrons.

$$\frac{d\sigma(pp \rightarrow pp)}{dt} = F_p^4(t) \quad (3)$$

where $F_p(t)$ and $F_\pi(t)$ are the proton and pion form factors, respectively, and $a_{qq}(t)$ is the elastic quark scattering amplitude.

Impressive arguments in favour of the additiveness of the interaction between dressed quarks are given by hadron-nucleus collisions. The quasi-nuclear hadron structure allows us to calculate the ratio of multiplicities of secondary hadrons in the central region for high energy NA and πA scatterings. At $A \rightarrow \infty$ this gives

$$\frac{\langle n_{ch} \rangle_{NA}}{\langle n_{ch} \rangle_{\pi A}} = \frac{3}{2}. \quad (4)$$

Accepting the hadron picture with two radii, we assume that hadrons are similar to light nuclei: the meson, consisting of a quark and an antiquark sufficiently far from each other reminds the deuteron while the baryon contains three constituent quarks in the same way as H_3 or He_3 is built up. The constituent quarks are surrounded by their "coat" of virtual particles. The radius of this "coat" is in fact the radius of the constituent quark. The mean distances between the constituent quarks determine the size of the hadron ([10]-[11], [16]).

The radius of the constituent quark can be estimated from the total hadron-hadron cross-section, which, as follows from Fig.1, can be expressed in terms of the total quark-quark cross-section. At moderately high energies $\sigma_{tot}(qq) \simeq 4,5mb$. Assuming that the total quark-quark cross section is determined by the geometrical sizes of the colliding quarks $\sigma_{tot}(qq) \simeq 2\pi(2r_q)^2$, we get

$$r_q^2 \simeq 0,5GeV^{-2}.$$

There is another way of obtaining the radius of the constituent quark in the framework of the parton hypothesis. Without going into details, we give here only the results: πp -scattering experiments [17] at moderately high energies $\sqrt{s} \simeq 40GeV$ lead to

$$r_q^2 \simeq 3\alpha'_p \simeq 0,45GeV^{-2}.$$

Hence, having $R_h^2 \simeq 17GeV^{-2}$,

$$\frac{r_q^2}{R_h^2} \simeq \frac{1}{30}.$$

(According to calculations compared to recent experimental data [18], the radius of the constituent quark turns out to be even smaller: $r_q^2 \approx 0,1GeV^{-2}$). We consider here, naturally, coloured quarks. Since the quark confinement is due to the colour forces, we are bound to accept the following hadron picture. (We will consider here a nucleon). At large momenta (but $P < 10^8 GeV/c$) the nucleon contains three clouds of quarks-partons (Fig.2a).

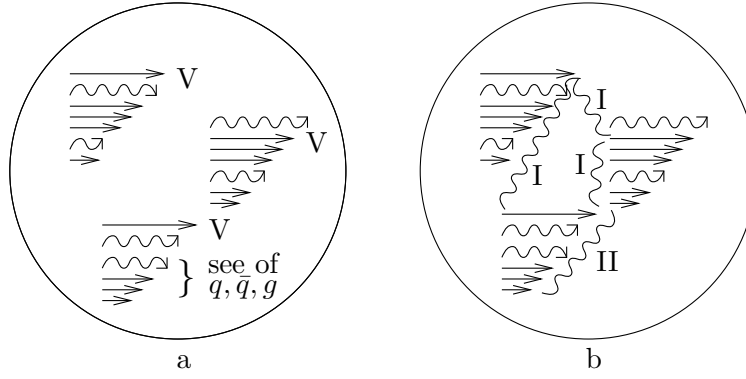


Fig.2

Each of the clouds contains a coloured quark-parton which carries the quantum numbers of the constituent quark, and a sea of quark-antiquark pairs and gluons, which is colourless and has zero quantum numbers. The gluon interaction which keeps the constituent quarks inside the hadrons is taking place between the fast components *I* [19] (Fig.2b). The gluon exchange is improbable between the partons *II* carrying a relatively small fraction of the momentum.

The transverse dimension of a cloud increases with the energy as $\sqrt{\alpha'_p \ln P/P_0}$, $P_0 \sim 10 \text{ GeV}/c$. Up to $P \ll 10^8 \text{ GeV}/c$, r_q remains essentially less than R_h and, practically, the three (or, in the case of a meson, two) clouds do not overlap³. When a fast hadron collides with the target, only one of the constituent quarks participates in the interaction; the other constituent quarks, or quark-parton clouds, remain spectators. The situation is different in the case of a hadron-nucleus interaction, i.e. when the target is large, and not only one, but two or three constituent quarks of the incident hadron can interact. We will come to this question later. As soon as $r_q^2 \ll R_h^2$, repeated collisions of the quarks are improbable. The interaction with the target is due to the slow components of the partons (a parton carrying energy E needs a time of the order of $\tau \sim E/\mu^2$ to interact). The quark-parton cloud the slow component of which participated in the interaction breaks into partons. These partons then, interacting with each other, obtain their own "coats" and become constituent (dressed) quarks, giving rise to the production of new particles (Fig.3).

³The case of overlapping quark-parton clouds may become important at RHIC energies. The presented approach is not suitable for handling this energy region

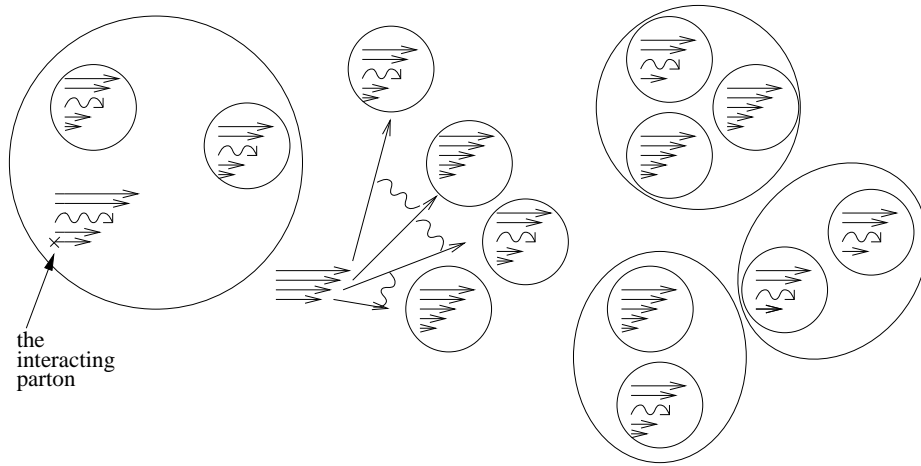


Fig.3

In the framework of the model, the three stages of the multiparticle production process are sufficiently well separated in time. The approach we are presenting deals in fact with the second and the third steps: the interactions of the partons and the gluons with each other which lead to the formation of constituent quarks, and the transition of these constituents into hadrons (mesons, baryons, meson and baryon resonances) in such a way that the set of hadron states corresponds to the states of the constituent quarks in the multiperipheral ladder.

The formation time of the constituent quark in its rest frame has to be determined by the quark radius r_q . A crucial point of our consideration is the assumption that the dressed quark exists long enough to interact repeatedly producing additional pairs of dressed quarks. One can assume that the resulting cloud of constituent quarks is "prepared" for hadronization. This means that every quark has suitable colour and flavour partners sufficiently close on the rapidity scale. Indeed, if there is a given quark for which partners suitable to form a hadron are too far on the rapidity scale, some additional quark-antiquark pairs will be produced so that the hadronization of all quarks becomes possible without any suppression. The same is true for colour excitations: if a quark has no suitable partners to form a white hadron state, then new quarks are produced, and the wrong colour is transferred to another rapidity region. This means that again, the transition of quarks into white hadron states takes place without any suppressing factors, and does not depend, e.g., on the probability of finding suitable partners for the quark. We call this property the soft hadronization and soft colour neutralization of the dressed quarks.

This approach is by no means the only possibility to handle the problem of the quark-hadron transfer. Our task is to present it and to demonstrate, why such a rough model may be justified and successful even now.

2 Multiparticle production processes

2.1 General description of the approach. The spectator mechanism

Considering a picture with quark confinement, one assumes the existence of two equivalent descriptions of the physical processes, namely: the description in terms of quark states

and that in terms of real particles, since each quark state corresponds to a set of hadron states.

Our aim is, in a sense, to translate the quark language into the hadron language. Dealing with soft processes (i.e. processes with small momentum transfer) and especially with inelastic scatterings at high energies, which lead to the production of many particles, we expect to have a large field for comparison with experiment.

The quark combinatorial calculus which has been proposed in [20],[21] provides a good possibility to handle the multiparticle production processes. Apart from the usual hypothesis about the quark structure of hadrons, two main assumption have been made. The first one concerned the spectator mechanism, which was based on the picture of spatially separated quarks. As we have told before, practically only one constituent quark of the incident hadron (and of the target) is taking part in the collision process, the other ones remain spectators. As a result of the collision, many new quarks are produced, which afterwards join the quark-spectators and form fast secondary hadrons, observable in experiment. Fig.4 shows a picture of meson-baryon and baryon-baryon collisions of this kind.

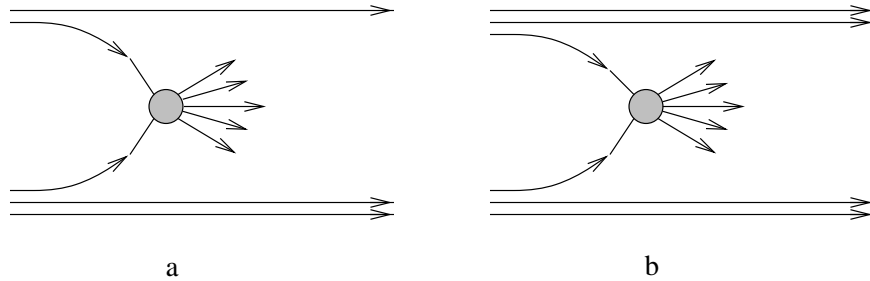


Fig.4

If the hadron consists of discrete "dressed" quarks, then inside a fast baryon each of them has to carry about 1/3 of the total baryon momentum, while inside a meson – about half of the meson momentum. Consequently, multiparticle production processes in hadron-hadron collisions can be divided into two, energetically different, regions: the central and the fragmentation ones (*I* and *II* in Fig.5).

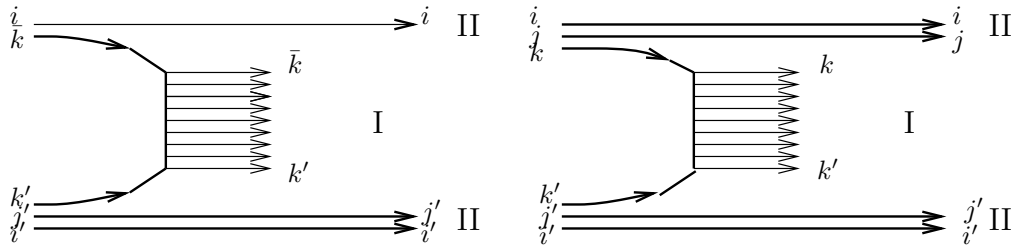


Fig.5

The quarks in the central region are sea-quarks, carrying a small fraction of the incident momentum. Joining each other, they form the spectrum of slow hadrons.

The quarks-spectators of the colliding particles (q_i, q_j and $q_{i'}, q_{j'}$ in Fig.5) join quarks (or antiquarks) of the sea forming the hadrons in the fragmentation region. The pair of

quarks q_k and $q_{k'}$ produced in the interaction "remember" their origin and have to be considered as belonging to the fragmentation region.

Let us see now, what processes are possible in the fragmentation region. (For the sake of simplicity we consider a baryon fragmentation process). The interacting quark q_k can join the spectators, forming a baryon state containing the same quarks as the incident one (Fig.6a). If the collision of q_i , q_j and q_k is coherent, then the produced hadron B_{ijk} is analogous to the initial state (in the case of an incident proton that means $p \rightarrow p$ transition). If the collision is not coherent, the produced B_{ijk}^* state is a superposition of possible real hadrons (e.g. $p \rightarrow p$, $p \rightarrow \Delta^+$ etc.).

The spectators q_i , q_j can join a sea quark; in this case a baryon state B_{ij} is formed (Fig.6b). At the same time q_k and a sea antiquark form a meson state M_k .

The baryon states B_{ijk} and B_{ij} carry about 2/3 of the momentum of the initial hadron. The interacting quark q_k carries away $x \sim 1/3$ (where $x = p_L/p_{max}$; p_L is the longitudinal momentum of the constituent quark, p_{max} that of the incident hadron). The longitudinal momentum of the newly produced quark q_k , which comes from the central region after the interaction, can be estimated assuming that quarks produced in the central region are distributed homogeneously in $\log x$, i.e. their longitudinal momenta follow the geometrical progression law. This is the so-called comb regime which leads to a Regge-pole exchange in elastic scattering. If so, the fastest produced quark has a momentum equal to one half of the incoming quark momentum, the next one 1/4 of it etc. This means that the meson state M_k is produced in the $x \leq 0,15$ region.

If one spectator joins two sea quarks, a baryon state B_i ($x \sim 1/3$) is formed; the other spectator joining a sea antiquark forms a meson state M_j ($x \sim 1/3$) (Fig.6c). There are also cases when only meson states are produced (Fig.6d,e).

The meson fragmentation process can be considered in the same way (Fig. 6f, g, h).

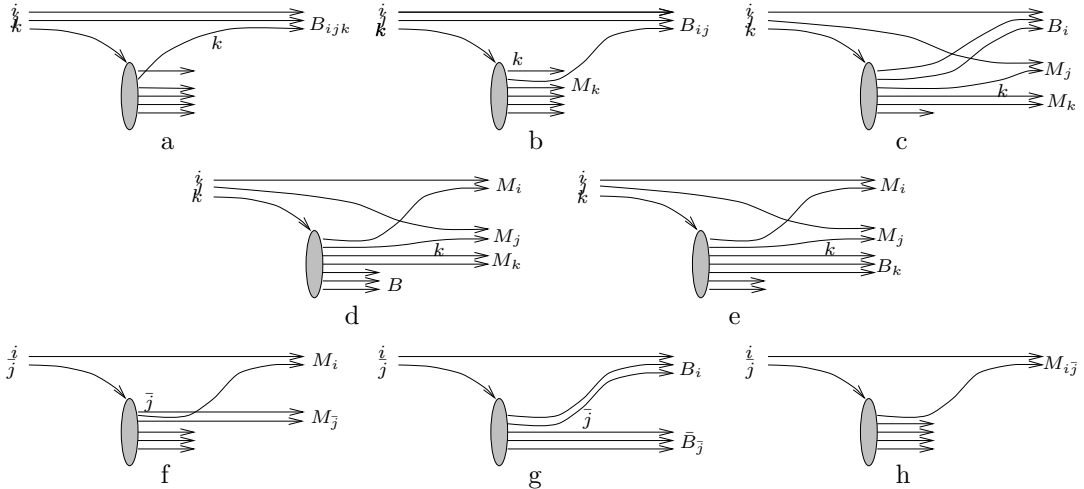


Fig.6

As it is seen, the spectator mechanism leads to the production of hadrons with a very definite momentum distribution. The comparison of the theoretical predictions with the experimental data shows a good agreement in different fields, such as resonance production in the region of secondaries with large momenta [30] or inclusive spectra of secondaries in pp and pA collisions [22],[23],[31].

2.2 Quark combinatorics

The second assumption made in the quark combinatorial calculus is connected with the newly produced particles. The classical quark model is $SU(6)$ symmetric. Hence, it is natural to assume that $SU(6)$ holds also for the production processes of secondary particles. This means that in the multiparticle production processes not only stable particles appear but also resonances, and the production probabilities of all hadron states belonging to one $SU(3)$ multiplet are equal⁴. Hence, the probability of the hadron production within one $SU(6)$ multiplet is proportional to the number of spin states of these hadrons, i.e. $2J + 1$.

In the framework of quark combinatorics it is assumed that hadrons are formed by quarks with small relative momenta, i.e. by neighbours on the rapidity axis. The quarks join each other with equal probability independently of their quantum numbers and of the fact if they are quarks or antiquarks.

In the central region, where the hadrons are formed by sea quarks only, an arbitrary particle might be with equal probability a quark or an antiquark: $1/2q + 1/2\bar{q}$. The nearest neighbour is again either a quark, or an antiquark. The probability of the states qq , $\bar{q}\bar{q}$ and $q\bar{q}$ is then

$$\left(\frac{1}{2}q + \frac{1}{2}\bar{q}\right) \left(\frac{1}{2}q + \frac{1}{2}\bar{q}\right) \rightarrow \frac{1}{4}qq + \frac{1}{4}\bar{q}\bar{q} + \frac{1}{2}q\bar{q} \rightarrow \frac{1}{4}qq + \frac{1}{4}\bar{q}\bar{q} + \frac{1}{2}M,$$

where $M = q\bar{q}$ is a meson state. Taking into account a third possible quark or antiquark, we get

$$\left(\frac{1}{4}qq + \frac{1}{4}\bar{q}\bar{q} + \frac{1}{2}M\right) \left(\frac{1}{2}q + \frac{1}{2}\bar{q}\right) \rightarrow \frac{1}{8}B + \frac{1}{8}\bar{B} + \frac{3}{4}M \left(\frac{1}{2}q + \frac{1}{2}\bar{q}\right),$$

where $B = qq$, $\bar{B} = \bar{q}\bar{q}$. Further iterations lead to the following multiplicity of particles produced in the central region:

$$(q, \bar{q} - sea) \rightarrow 6N \cdot M + N \cdot B + N \cdot \bar{B}. \quad (5)$$

The number N depends on the total energy of the colliding particles, and increases with the growth of s . Supposing that the multiplicity $N(s)$ is increasing logarithmically, it is convenient to write

$$N(s) = b \ln \frac{s}{s_0}$$

at asymptotic energies. The parameters b and s_0 cannot be determined by quark combinatorics, but have to be the same for all processes. Hence, the relation between the produced mesons M , baryons B and antibaryons \bar{B} is [20]

$$M : B : \bar{B} = 6 : 1 : 1. \quad (6)$$

In the same way one can get relations between baryons and mesons in the fragmentation region [26]. In this case we consider an incident quark q_i which, joining a quark or an

⁴ There are some particles which do not fit into this scheme; their properties seem to be due to the dynamics of the quark confinement [24]. Due to [25], there are two sorts of light quarks: constituent quarks with masses about 300 MeV and much lighter relativistic current quarks. This means that we have to take into account two different types of bound states. If a constituent quark is combined into a meson, then due to its small mass difference compared to the strange quark we find an approximate $SU(3)$ flavour symmetry in the corresponding mesonic spectrum. If the current quark is used to build a meson, then scalar or pseudoscalar mesons are created that have nothing to do with $SU(3)$ symmetry

antiquark of the sea, forms mesons or baryons containing this quark with the probability 2 : 1:

$$(q_i + q, \bar{q} - sea) \rightarrow \frac{1}{3}B_i + \frac{2}{3}M_i + \frac{1}{3}M + N(s)(6M + B + \bar{B}). \quad (7)$$

Here $B_i = q_iqq$, $M_i = q_i\bar{q}$; $N(s)$ is a large number which is characterized by the number of quarks in the sea.

A similar relation is valid for the case when a pair of quarks q_iq_j transforms into hadrons:

$$(q_i + q, \bar{q} - sea) \rightarrow \frac{1}{2}B_{ij} + \frac{1}{12}(B_i + B_j) + \frac{5}{12}(M_i + M_j) + \frac{1}{6}M + N(s)(6M + B + \bar{B}). \quad (8)$$

The baryon state B_{ij} contains both incident quarks: $B_{ij} = q_iq_jq$.

Supposing that quarks q_i, q_j and the quark q_k (Fig.5) form hadrons in an independent way, the relations (7) and (8) provide a possibility to find the relative weight of the fragmentation processes in Fig.6b, 6c and 6e: 1/2 : 1/12 : 1/3 . The probability of the process 6a can not be obtained in the framework of quark combinatorics.

Hence, if a quark q_k belonging to the baryon B_{ijk} hits the target, fast particles are produced with the following probabilities [27]:

$$\begin{aligned} B_{ijk} \rightarrow & \\ & \Delta B_{ijk} + \Delta^* B_{ijk}^* + (1 - \Delta - \Delta^*) \left[\frac{1}{2}B_{ij} + \frac{1}{12}(B_i + B_j) + \right. \\ & \left. + \frac{5}{12}(M_i + M_j) + \frac{1}{3}B_k + \frac{2}{3}M_k + \frac{1}{2}M \right] + \dots \end{aligned} \quad (9)$$

Here Δ and Δ^* are the probabilities of the coherent and incoherent transitions $B_{ijk} \rightarrow B_{ijk}$ and $B_{ijk} \rightarrow B_{ijk}^*$, respectively; they have to be determined from the experiment. (The contribution of hadrons produced in the central region is absent in this expression).

Similarly, the probability of the production of fast hadrons after the collision of a meson $M_{i\bar{j}}$ with the target is

$$\begin{aligned} M_{i\bar{j}} \rightarrow & \\ & \delta M_{i\bar{j}} + \delta^* M_{i\bar{j}}^* + \\ & + (1 - \delta - \delta^*) \left[\frac{1}{3}(B_i + \bar{B}_{\bar{j}}) + \frac{2}{3}(M_i + M_{\bar{j}}) + \frac{2}{3}M \right] + \dots \end{aligned} \quad (10)$$

Here the probabilities δ and δ^* of the processes $M_{i\bar{j}} \rightarrow M_{i\bar{j}}$ and $M_{i\bar{j}} \rightarrow M_{i\bar{j}}^*$ cannot be defined in the framework of quark combinatorics. The probabilities Δ , Δ^* and δ , δ^* can depend on the initial hadron and on the type of the collision, thus in fact one has to write $\Delta_p(pp)$, $\Delta_p(Kp)$, $\delta_K(Kp)$ and so on. For the sake of simplicity, we will neglect this.

Let us mention that the presented relations, and (6) and (7) in particular, were obtained without taking into account the colour degrees of freedom of the quarks. Having in mind that quarks are coloured objects, the method [20]-[21] which leads to these results can be understood in the following way. It is, practically, supposed that there are strong colour correlations between the quarks in the process when they join each other to form hadrons. These correlations provide automatically the colour combinations necessary for the production of white states.

Indeed, as we have said already, in quark combinatorics it is assumed that quarks which join each other to form hadrons appear accidentally as neighbours on the rapidity

axis. If, however, the colour states are not taken into account, hadron states can be formed only if these quarks have the proper colours; inside small domains there occur white groups of quarks, all the other quantum numbers of which are arbitrary. This additional assumption of colour correlation is a very strong one, which cannot be a rigid condition for the production of hadron states. It is therefore interesting to understand what could be the consequences of the absence of colour correlations.

In [28] we consider the situation when the quarks and antiquarks which are close to each other on the rapidity axis, have uncorrelated, arbitrary colours. It turns out that quark combinatorics for coloured quarks does not determine unambiguously the relation between the number of baryon and meson states either in the central region, or in the fragmentation region. This relation is a function of a parameter α characterizing the diffusion of quarks along the rapidity axis and their formation into hadrons. If, however, the relation (7) is satisfied, we obtain $M : B : \bar{B} \simeq 5, 2 : 1 : 1$. In other words, the fact that there is strong colour correlation or no colour correlation has only little impact on the ratio of mesons and baryons in the central region. (We interpret $q \rightarrow 1/3B + 2/3M$ as a relation expressing that the baryon number of the quark manifests itself as the probability of the production of a baryon state by this quark).

Let us see the case of quarks with uncorrelated colours in more detail. The main feature of quark-hadron transitions in this case is that only a few white states appear on a small interval of the rapidity axis: in a set of nine states this is only one colour singlet $1/\sqrt{3}q_i\bar{q}_i$ ($i = 1, 2, 3$ are the colour indices). In a system of three quarks qqq only one of 27 states is white: the totally antisymmetric colour state $1/\sqrt{6}\varepsilon_{ijk}q_iq_jq_k$. The small relative probability of a transition to white states is the reason why the quarks formed in the interaction process cannot be transformed into hadrons immediately, but only in the course of many stages. Only white states of quarks combine into hadrons, while the quarks that have not found suitable partners inside the small domain will diffuse, interacting with each other, along the rapidity axis. Only after many "collisions" will these quarks find partners for the formation of white states. In fact the picture of quarks with uncorrelated colours which form hadrons as the result of repeated interactions is much closer to the spirit of "soft" quark confinement.

The peculiarity of this approach is the formation of antisymmetric colour states of two quarks $\frac{1}{\sqrt{2}}\varepsilon_{ijk}q_jq_k$ – diquarks (we shall denote these states as $(\hat{q}q)_i$). However, inside a small domain such states may not find a suitable partner to form a baryon. But they are, in fact, parts of real baryons, thus we have to assume that they remain "bound" states which also diffuse along the rapidity axis.

If the quarks are formed as a result of repeated "collisions", this explains why the quarks must be in a statistical equilibrium before they can form hadrons. Hence, in our calculations we assume that the probability to find a quark, an antiquark, a diquark or an antidiquark in the sea is determined by constants. If the probability to find a diquark or an antidiquark is α , that of a quark or an antiquark is $(1 - \alpha)$:

$$(1 - \alpha)\frac{1}{2}(q + \bar{q}) + \alpha\frac{1}{2}(\hat{q}q + \hat{\bar{q}}\bar{q}) \quad (11)$$

where we omitted the colour indices; in fact $q = \frac{1}{3} \sum_{i=1}^3 q_i$ and $\hat{q}q = \frac{1}{3} \sum_{i=1}^3 (\hat{q}q)_i$. The condition of the equilibrium means that after the collision of two systems of the type (11) hadrons,

quark and diquark states are formed in the same proportions as in (11), i.e.

$$\begin{aligned} & [(1 - \alpha)\frac{1}{2}(q + \bar{q}) + \alpha\frac{1}{2}(\hat{q}q + \hat{\bar{q}}\bar{q})][(1 - \alpha)\frac{1}{2}(q + \bar{q}) + \alpha\frac{1}{2}(\hat{q}q + \hat{\bar{q}}\bar{q})] \\ & \rightarrow \text{hadrons} + a\frac{1}{2}(q + \bar{q}) + \frac{1}{2}(\hat{q}q + \hat{\bar{q}}\bar{q}); \end{aligned} \quad (12)$$

here

$$\frac{b}{a} = \frac{\alpha}{1 - \alpha}. \quad (13)$$

Further, we will assume that only the nearest neighbours form hadrons. This does not alter, of course, the result (such an assumption is rather the definition of what is a "neighbour"), but it simplifies the calculations. In addition, let us suppose that the diquarks do not form bound states forever, but dissociate with a probability X into constituent quarks.

Thus, if two quarks turn out to be the nearest neighbours, the probability to form a diquark is $1/3$:

$$qq \rightarrow 1/3\hat{q}q + 2/3q \cdot q. \quad (14)$$

We denote here by $q \cdot q$ a quark pair which does not form a diquark.

If the nearest neighbours are a quark and an antiquark, then

$$q\bar{q} \rightarrow 1/9M + 8/9q \cdot \bar{q}, \quad (15)$$

where M is a meson (a white state of $q\bar{q}$). If a diquark is "colliding" with a quark, a baryon state B is formed with a probability $1/9$:

$$\hat{q}qq \rightarrow 1/9B + 8/9\hat{q}q \cdot q, \quad (16)$$

and, similarly,

$$\hat{q}q\bar{q} \rightarrow 1/9M \cdot q + 8/9\hat{q}q \cdot \bar{q}. \quad (17)$$

The collisions of two diquarks or of a diquark and an antidiquark result in the following states:

$$\hat{q}q\hat{q}q \rightarrow 2/9B \cdot q + 7/9\hat{q}q \cdot \hat{q}q, \quad (18)$$

$$\hat{q}q\hat{\bar{q}}\bar{q} \rightarrow 1/9q \cdot M \cdot \bar{q} + 8/9\hat{q}q \cdot \hat{\bar{q}}\bar{q}. \quad (19)$$

The relations (16)-(19) lead to

$$\begin{aligned} & \left[\frac{1 - \alpha}{2}(q + \bar{q}) + \frac{\alpha}{2}(\hat{q}q + \hat{\bar{q}}\bar{q}) \right] \left[\frac{1 - \alpha}{2}(q + \bar{q}) + \frac{\alpha}{2}(\hat{q}q + \hat{\bar{q}}\bar{q}) \right] \rightarrow \\ & \frac{1}{2}(q + \bar{q})\frac{1}{9}(-\alpha^2 - 11\alpha + 14) + \\ & \frac{1}{2}(\hat{q}q + \hat{\bar{q}}\bar{q})\frac{1}{18}(\alpha^2 + 26\alpha + 3) + \frac{1}{18}M + \frac{1}{18}B + \frac{1}{18}\bar{B}. \end{aligned} \quad (20)$$

The number of baryons (antibaryons) and mesons in the sea (in the central region) is determined by the relation (20):

$$B/M = \alpha, \quad \bar{B}/M = \alpha. \quad (21)$$

This means that the proportions of baryons (antibaryons) and mesons are the same as the probability to find a diquark (or an antidiquark) in the sea. Depending on the value of α , this can vary between 0 and 1. The parameter α can be fixed if we assume that the fragmentation probability of the quark is determined by (7).

Let us consider now the process of meson and baryon formation by a tagged quark q' . If this quark "collides" with coloured quarks and diquarks of the sea, white states containing this quark are formed: $M' = q'\bar{q}$ and $B' = q'qq$. We shall denote by c the probability to form a meson state M' , by d that to form a baryon state B' . These probabilities depend on the ratio of the numbers of quarks and diquarks in the sea, i.e. on α :

$$q' + \text{sea } q, \bar{q}, \hat{q}q, \hat{q}\bar{q} \rightarrow c(\alpha)M' + d(\alpha)B',$$

$$c(\alpha) + d(\alpha) = 1. \quad (22)$$

A single "collision" of q' with quarks and diquarks of the sea leads to

$$q' \left[\frac{1-\alpha}{2}(q + \bar{q}) + \frac{\alpha}{2}(\hat{q}q + \hat{q}\bar{q}) \right] \rightarrow \frac{1}{18}[2(7 + \alpha) +$$

$$+ 3X(1 - \alpha)]q' + (1 - X)\frac{1}{6}(1 - \alpha)\hat{q}q' + \frac{1}{18}M' + \frac{\alpha}{18}B'. \quad (23)$$

As before, the coefficients of M' , B' , q' and $\hat{q}q'$ correspond to the probabilities of the transition of the quark q' to these states. Calculating these probabilities, we have used the relations

$$q'q \rightarrow 1/3\hat{q}q' + 2/3q' \cdot q,$$

$$q'\bar{q} \rightarrow 1/9M' + 8/9q' \cdot \bar{q},$$

$$q'\hat{q}q \rightarrow 1/9B' + 8/9q' \cdot \hat{q}q,$$

$$q'\hat{q}\bar{q} \rightarrow 1/9M' \cdot \bar{q} + 8/9q' \cdot \hat{q}\bar{q}. \quad (24)$$

As we see, after the first "collision" diquark states containing q' appear. The "collision" of these diquarks with quarks and diquarks of the sea leads to the transition

$$\hat{q}q' \left[\frac{1-\alpha}{2}(q + \bar{q}) + \frac{\alpha}{2}(\hat{q}q + \hat{q}\bar{q}) \right] \rightarrow \frac{1}{36}[1 + \alpha + 3X(16 - \alpha)]q' +$$

$$+(1 - X)\frac{1}{18}(16 - \alpha)\hat{q}q' + \frac{1}{36}M' + \frac{\alpha}{36}(2 + \alpha)B'. \quad (25)$$

The probabilities c and d are results of repeated "collisions" of quarks with subsequent transitions of the type (23), and of "collisions" of the appearing diquarks with subsequent transitions (25). Fig.7 shows the ratio $c(\alpha)/d(\alpha)$ as a function of α .

At the value $\alpha \simeq 0,194$ the probabilities of baryons B' and mesons M' are determined by the relation (7), and (20) leads to

$$M : B : \bar{B} \simeq 5, 2 : 1 : 1. \quad (26)$$

Thus, if $q' \rightarrow 1/3B' + 2/3M'$ is satisfied (which can be considered as the "local" baryon charge conservation), the ratio of the number of produced mesons, baryons and antibaryons is pretty stable.

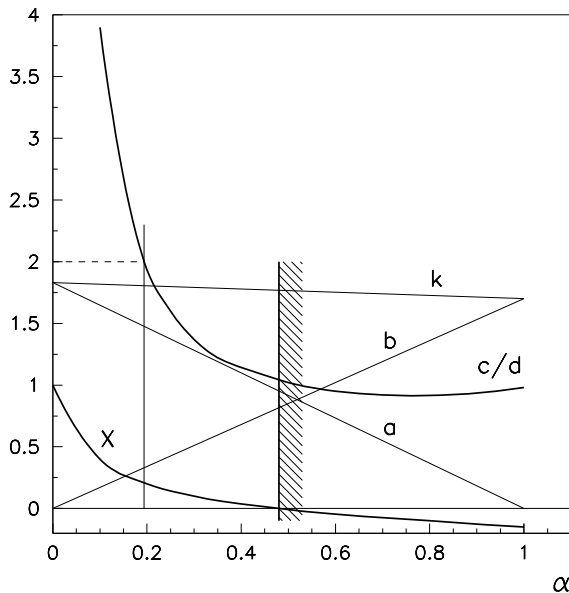


Fig.7

2.3 Probabilities of the production of hadron states in the central and fragmentation regions

It is a well-known experimental fact that in multiparticle production processes the production of strange quarks is suppressed. According to that, it was proposed [20] to consider a non-symmetrical quark sea with a relatively suppressed production of strange quarks:

$$u\bar{u} : d\bar{d} : s\bar{s} = 1 : 1 : \lambda. \quad (27)$$

This suppression is characterized by a parameter $0 \leq \lambda \leq 1$. In the case of $\lambda = 1$ the symmetry between the quarks u, d, s is restored.

To be in a position to compare (9) and (10) with the experimental data, we face here the question what means M and B , what real hadrons correspond to the mesonic and baryonic states B_{ij}, B_i, M_i etc. Indeed, quark combinatorics, while operating with constituent quark states $q\bar{q}$ and qqq does not answer the question by what real particles they are saturated. In [20] the dominance of the lowest $SU(6)$ multiplets was supposed, i.e. the meson 1+35-plet ($J^P = 0^{-1}, 1^{-1}$) for the $q\bar{q}$ states and the baryon 56-plet ($J^P = 1/2^+, 3/2^+$) for qqq , respectively. This is a rather rough approach, and, of course, a contribution of hadrons belonging to higher multiplets is quite natural.

The determination of hadrons saturating the meson and baryon states is in fact an experimental question which, in a sense, characterizes the quark confinement. The analysis of experimental data shows that the contribution of hadrons with $L=1$ is significant, 20-30 % of the produced particles ([42],[43]). The share of $L=2$ multiplets seems to be about 5-10 % (see [43],[44]).

In the process of hadronization white states $q\bar{q}$ and qqq are produced. The decomposition of the production amplitude of these white states into hadronic wave functions determines the content of M and B . In general, we can write

$$\begin{aligned} M_i &= \alpha_i(1)M_i(1) + \alpha_i(0)M_i(0), \\ M &= \alpha(1)M(1) + \alpha(0)M(0). \end{aligned} \quad (28)$$

The indices $L = 0, 1$ correspond to the s and p -wave states, respectively. The probabilities $\alpha_i(L)$ and $\alpha(L)$ are fixed by the conditions $\alpha_i(1) + \alpha_i(0) = 1$, $\alpha(1) + \alpha(0) = 1$.

In a more general form one can write

$$\begin{aligned} M &= \sum_L \mu_L M_L, \\ M_i &= \sum_L \mu_L^{(i)} M_L^{(i)} \end{aligned} \quad (29)$$

The real hadron content of the states B and B_i is defined as

$$\begin{aligned} B &= \sum_L \beta_L B_L, \\ B_i &= \sum_L \beta_L^{(i)} B_L^{(i)}. \end{aligned} \quad (30)$$

Here L defines the multiplet, while the coefficients μ_L , $\mu_L^{(i)}$ and β_L , $\beta_L^{(i)}$ are production probabilities of mesons and baryons of the given multiplet in the process of quark hadronization. These probabilities are determined by characteristic relative momenta of the quarks which join each other, or rather by their invariant masses $\sum_i (m_i^2 + k_{i\perp}^2)/x_i(1 - x_i)$.

Graphically, the colour neutralization of meson and baryon states can be represented as it is shown on Fig.8.

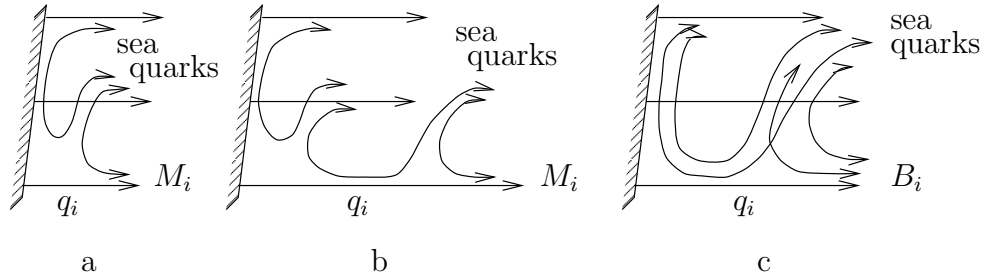


Fig.8

2.4 Multiplicities of the secondary particles in the central and fragmentation regions

We shall give here expressions for the multiplicities of secondary particles in both the fragmentation and the central regions [27]. We consider the cases of incident proton, Λ and Σ^+ hyperons, π^+ and K^+ mesons. Expressions for other incident particles can easily be obtained from these ones. For example, the case of a neutron can be obtained from that of a proton by isotopic reflection, i.e. substituting $p \leftrightarrow n$, $\Delta^{++} \leftrightarrow \Delta^-$, $\pi^+ \leftrightarrow \pi^-$, $K^+ \leftrightarrow K^0$. In the case of an initial antiparticle one has to carry out charge conjugation $p \leftrightarrow \bar{p}$, $\Delta^{++} \leftrightarrow \bar{\Delta}^{--}$ etc.

The relations (9) and (10) and the expressions of B_{ij} , M_i , B_i in terms of the real hadrons allow us to get the fragmentation multiplicities easily. For this purpose we have to take the wave function of the incident particle and to consider all possible interactions of its constituents.

As an example, let us consider in detail the fragmentation of the proton. We assume that the incident proton is completely polarized (this fact is of no significance from the point of view of the result). The proton wave function in this case is

$$\Psi(p^\uparrow) = \sqrt{\frac{2}{3}}\{u^\uparrow u^\uparrow d^\downarrow\} - \sqrt{\frac{1}{3}}\{u^\uparrow u^\downarrow d^\uparrow\}.$$

It is implied that the functions are symmetrized with respect to the $SU(6)$ indices, e.g.

$$\{u^\uparrow u^\uparrow d^\downarrow\} = \sqrt{\frac{1}{3}}(u^\uparrow u^\uparrow d^\downarrow + u^\uparrow d^\downarrow u^\uparrow + d^\downarrow u^\uparrow u^\uparrow).$$

It can be seen immediately that for the quarks-spectators the probability of being in a $\{u^\uparrow u^\uparrow\}$ is $2/9$ (while the quark d^\downarrow is interacting), in $\{u^\uparrow u^\downarrow\}$ it is $1/9$, in $\{u^\uparrow d^\uparrow\}$ also $1/9$. When the quark u^\uparrow is interacting, the spectators are in a state

$$\frac{1}{\sqrt{5}}(2\{u^\uparrow d^\downarrow\} - \{u^\downarrow d^\uparrow\}) \equiv (ud)_p.$$

Thus, we have

$$B_{ij} = \frac{2}{9}B(u^\uparrow u^\uparrow) + \frac{1}{9}B(u^\uparrow u^\downarrow) + \frac{1}{9}B(u^\uparrow d^\uparrow) + \frac{5}{9}B_p(ud).$$

The decompositions of $B(u^\uparrow u^\uparrow)$ and $B(u^\uparrow u^\downarrow)$ into the real hadrons of the 56-plet lead to identical results, and therefore we write

$$\frac{1}{9}B(u^\uparrow u^\downarrow) + \frac{2}{9}B(u^\uparrow u^\uparrow) = \frac{1}{3}B(uu).$$

For the sake of simplicity we introduce the notation $B(u^\uparrow d^\uparrow) = B_1(ud)$. In the case of an incident proton the states B_i and M_i are

$$B_i = \frac{2}{3}B(u) + \frac{1}{3}B(d) \quad \text{and} \quad M_i = \frac{2}{3}M(u) + \frac{1}{3}M(d),$$

respectively. As a result, we can write

$$\begin{aligned} p &\rightarrow \Delta_p \cdot p + \Delta_p^* \cdot B_p^* + \\ &+ (1 - \Delta_p - \Delta_p^*) \left\{ \frac{1}{2} \left[\frac{5}{9}B_p(ud) + \frac{1}{3}B(uu) + \frac{1}{9}B_1(ud) \right] + \right. \\ &+ \left. \frac{1}{2} \left[\frac{2}{3}B(u) + \frac{1}{3}B(d) \right] \right\} + \frac{3}{2} \left[\frac{2}{3}M(u) + \frac{1}{3}M(d) \right]. \end{aligned} \quad (31)$$

Expanding the right-hand side in terms of the hadron states h (i.e. the meson states $h_{M(L)}$ and the baryon states h_B) we, finally, obtain

$$\begin{aligned} p &\rightarrow \Delta_p \cdot p + \\ &+ \sum_h h_B \left\{ \Delta_p^* \cdot \beta_h(p) + (1 - \Delta_p - \Delta_p^*) \left[\frac{5}{18}\beta_h(ud_p) + \right. \right. \\ &+ \left. \frac{1}{6}\beta_h(uu) + \frac{1}{18}\beta_h(ud_1) + \frac{1}{3}\beta_h(u) + \frac{1}{6}\beta_h(d) \right] \right\} + \\ &+ (1 - \Delta_p - \Delta_p^*) \sum_L \sum_h h_{M(L)} \alpha_i(L) \left[\mu_h^L(u) + \frac{1}{2}\mu_h^L(d) \right] \end{aligned} \quad (32)$$

or

$$p \rightarrow \sum_h F_h(p) \cdot h, \quad (33)$$

where $F_h(p)$ denotes the multiplicity of the secondary proton in the fragmentation region. Similarly, the multiplicities of Λ and Σ^+ hyperons in the fragmentation region are

$$\begin{aligned} \Lambda \rightarrow \sum_h F_h(\Lambda) \cdot h = & \\ & = \Delta_\Lambda \cdot \Lambda + \sum_h h_B \left\{ \Delta_\Lambda^* \cdot \beta_h(\Lambda) + (1 - \Delta_\Lambda - \Delta_\Lambda^*) \left[\frac{\xi}{2(2+\xi)} \beta_h(ud_\Lambda) + \right. \right. \\ & + \frac{1}{4(2+\xi)} (\beta_h(us_1) + \beta_h(ds_1) + \beta_h(us_0) + \beta_h(sd_0)) + \\ & \left. \left. + \frac{1+2\xi}{6(2+\xi)} \beta_h(s) + \frac{5+\xi}{12(2+\xi)} (\beta_h(u) + \beta_h(d)) \right] \right\} + \\ & + (1 - \Delta_\Lambda - \Delta_\Lambda^*) \sum_L \sum_h h_{M(L)} \alpha_i(L) \left[\frac{5+4\xi}{6(2+\xi)} \mu_h^L(s) + \right. \\ & \left. \frac{5\xi+13}{12(2+\xi)} (\mu_h^L(u) + \mu_h^L(d)) \right] \end{aligned} \quad (34)$$

and

$$\begin{aligned} \Sigma^+ \rightarrow \sum_h F_h(\Sigma^+) \cdot h = & \\ & = \Delta_\Sigma \cdot \Sigma^+ + \sum_h h_B \left\{ \Delta_\Sigma^* \cdot \beta_h(\Sigma^+) + (1 - \Delta_\Sigma - \Delta_\Sigma^*) \left[\frac{\xi}{2(2+\xi)} \beta_h(uu) + \right. \right. \\ & + \frac{5}{6(2+\xi)} \beta_h(us_\Sigma) + \frac{1}{6(2+\xi)} \beta_h(us_1) + \frac{\xi+5}{6(2+\xi)} \beta_h(u) + \frac{1+2\xi}{6(2+\xi)} \beta_h(s) \left. \right] \right\} + \\ & + (1 - \Delta_\Sigma - \Delta_\Sigma^*) \sum_L \sum_h h_{M(L)} \alpha_i(L) \left[\frac{5\xi+13}{6(2+\xi)} \mu_h^L(u) + \frac{5+4\xi}{6(2+\xi)} \mu_h^L(s) \right]. \end{aligned} \quad (35)$$

Contrary to the proton case, in (34) and (35) it is taken into account that the cross section of the interaction is less for the strange quark than for the non-strange one. Their ratio $\xi = \sigma_{inel}(sq)/\sigma_{inel}(qq)$ is close to 2/3.

Formula (10) enables us to calculate the fragmentation secondaries for incident mesons. In the cases π^+ and K^+ we get, as follows,

$$\begin{aligned} \pi^+ \rightarrow \sum_h F_h(\pi^+) \cdot h = & \delta_\pi \cdot \pi^+ \\ & + \sum_L \sum_h h_{M(L)} \cdot \alpha_i(L) \left\{ \delta_\pi^* \mu_h^L(\pi^+) + (1 - \delta_\pi - \delta_\pi^*) \left[\frac{2}{3} \mu_h^L(u) + \frac{2}{3} \mu_h^L(\bar{d}) \right] \right\} + \\ & + \sum_h h_B (1 - \delta_\pi - \delta_\pi^*) \frac{1}{3} \beta_h(u) + \sum_h h_{\bar{B}} (1 - \delta_\pi - \delta_\pi^*) \frac{1}{3} \beta_h(\bar{d}), \end{aligned} \quad (36)$$

$$\begin{aligned} K^+ \rightarrow \sum_h F_h(K^+) \cdot h = & \delta_K \cdot K^+ \\ & + \sum_L \sum_h h_{M(L)} \cdot \alpha_i(L) \left\{ \delta_K^* \mu_h^L(K^+) + (1 - \delta_K - \delta_K^*) \left[\frac{2}{3} \mu_h^L(u) + \frac{2}{3} \mu_h^L(\bar{s}) \right] \right\} + \\ & + \sum_h h_B (1 - \delta_K - \delta_K^*) \frac{1}{3} \beta_h(u) + \sum_h h_{\bar{B}} (1 - \delta_K - \delta_K^*) \frac{1}{3} \beta_h(\bar{s}). \end{aligned} \quad (37)$$

In (36, 37) the parameter ξ does not occur because, due to (9), the secondary hadron content of the quark-spectator is equal to that of the quark which underwent interaction.

In the central region the multiplicity of secondary particles is given by (5). Due to the additive quark model, the energy which is used for the production of the new (sea) quarks is determined by the energy of the colliding quarks. In the pion-nucleon collision the energy squared is about 1/6, in nucleon-nucleon collision about 1/9 of the total energy of hadrons. That means that in the case of pion-nucleon collision we have

$$N_{\pi N}(s) = b \ln \frac{s}{6s_0} = b \ln \frac{s}{s_{\pi N}^0}, \quad (38)$$

while for the nucleon-nucleon case

$$N_{NN}(s) = b \ln \frac{s}{9s_0} = b \ln \frac{s}{s_{NN}^0}. \quad (39)$$

In the collision processes of strange particles one has to remember the difference between the cross sections of the interaction of strange and non-strange quarks, and the fact that the heavier strange quark takes away a larger fraction of the hadron momentum. Hence, for the kaon-nucleon collision one can write

$$N_{KN}(s) = \frac{b\xi}{1+\xi} \ln \frac{s}{3(1+\mu)s_0} + \frac{b}{1+\xi} \ln \frac{s\mu}{3(1+\mu)s_0} = b \ln \frac{s}{S_{KN}^0}, \quad (40)$$

where $\mu = \frac{m_q}{m_s} \approx \frac{2}{3}$ is the ratio of the strange and non-strange quarks. Finally,

$$N_{\Lambda N}(s) = N_{\Sigma N}(s) = \frac{2b}{2+\xi} \ln \frac{s\mu}{3(1+2\mu)s_0} + \frac{\xi b}{2+\xi} \ln \frac{s}{3(1+2\mu)s_0} = b \ln \frac{s}{S_{\Lambda N}^0}. \quad (41)$$

The obtained expressions give a possibility to calculate the absolute values of average multiplicities of secondary particles in hadron-hadron collisions. The parameters are fitted to the experimental data and according to them the coefficients in (38-41) are calculated [27]. (For example, the value of λ is selected to give the best agreement with the experimental K/π ratio in the central region and is found to be 0,3). Supposing that the probabilities Δ and δ of the coherent processes $B_{ijk} \rightarrow B_{ijk}$ and $M_{i\bar{j}} \rightarrow M_{i\bar{j}}$ are mostly of diffractive origin, the value of these probabilities is estimated using the data on diffraction scattering. In the additive quark model the cross sections of diffraction processes in the meson-nucleon and baryon-nucleon scatterings are determined by the diagrams in Fig.9.

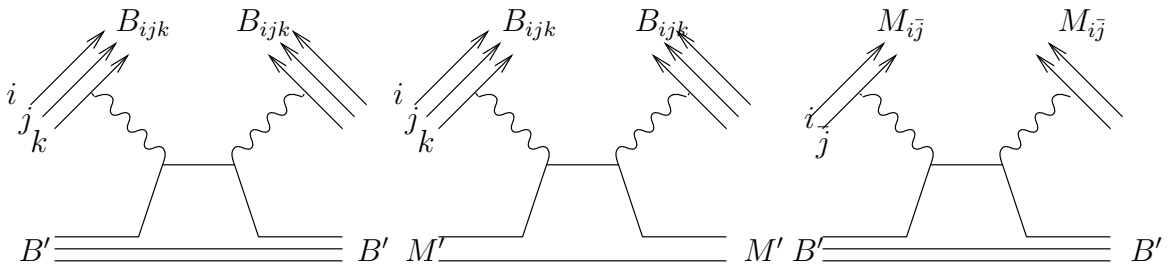


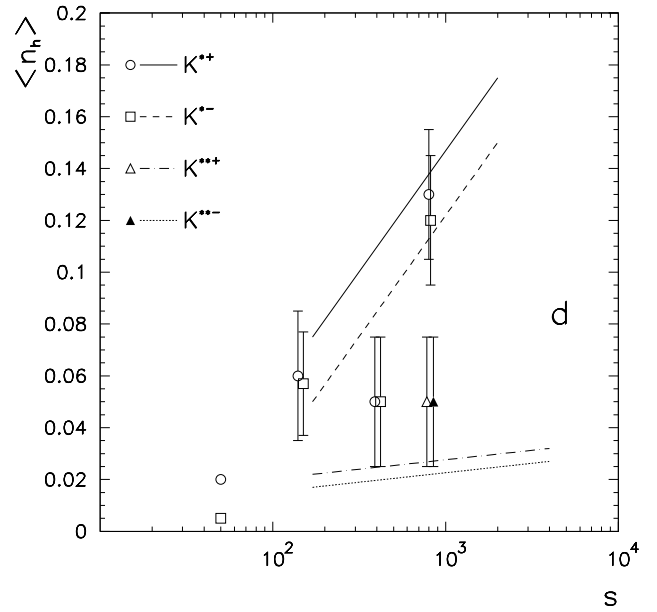
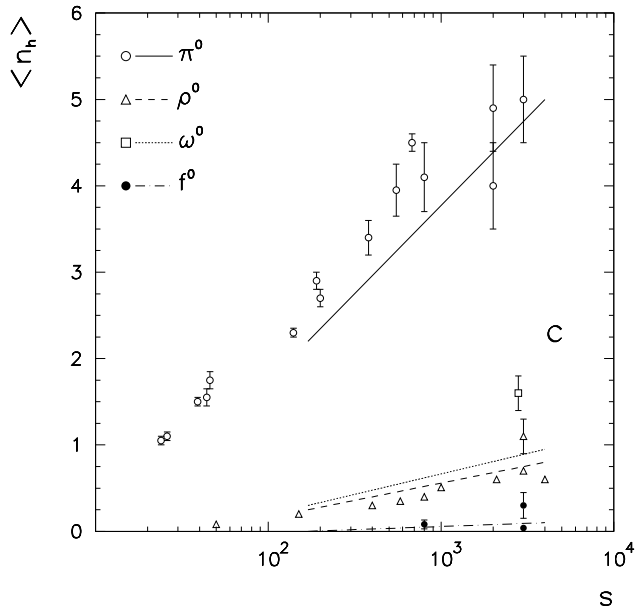
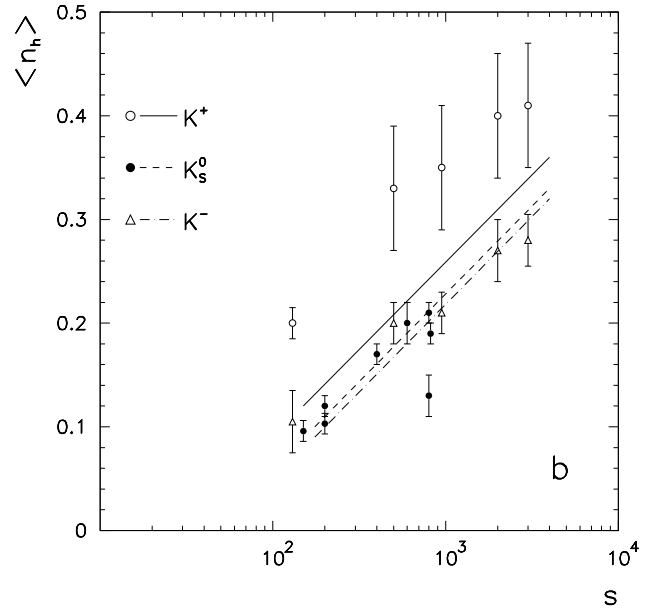
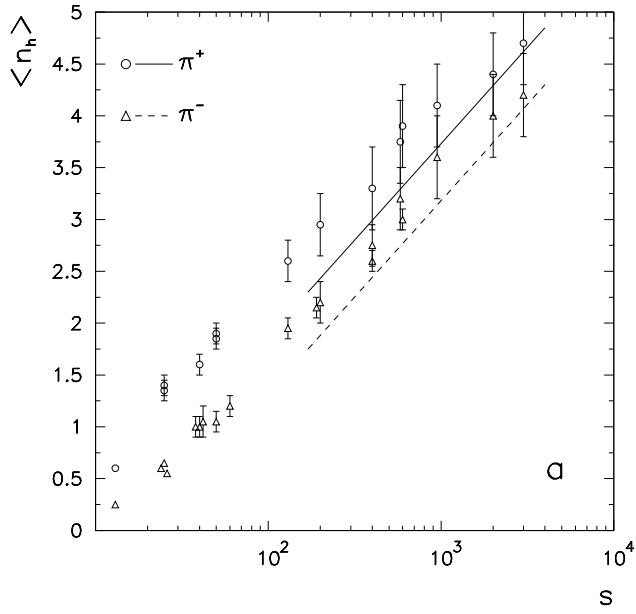
Fig.9

(For the values of Δ and δ , see [27]).

Experimental data on average multiplicities of secondary hadrons in the pp , πp and Kp collisions permit us to prove the basic statements of quark combinatorics.

Consider first the meson production processes. In Figs.10-12 the data on average multiplicities of secondary mesons in pp (Fig.10), $\pi^\pm p$ (Fig.11) and $K^- p$ (Fig.12) collisions are presented. The straight lines correspond to the predictions of the quark combinatorial calculus. In each case there is a satisfactory agreement between theory and experiment.

Concerning baryons and baryon resonances, the experimental data and the corresponding predictions of the quark model agree only roughly. E.g., the ratios Λ/Σ^0 , $\Sigma^+(1385)/\Sigma^0$ and $\Sigma^-(1385)/\Sigma^0$ satisfy the prediction quite well, what corresponds to the idea of baryons produced in $SU(6)$ multiplets. The same ratios indicate that there might be a significant contribution of higher resonances. (For details, see [27]).



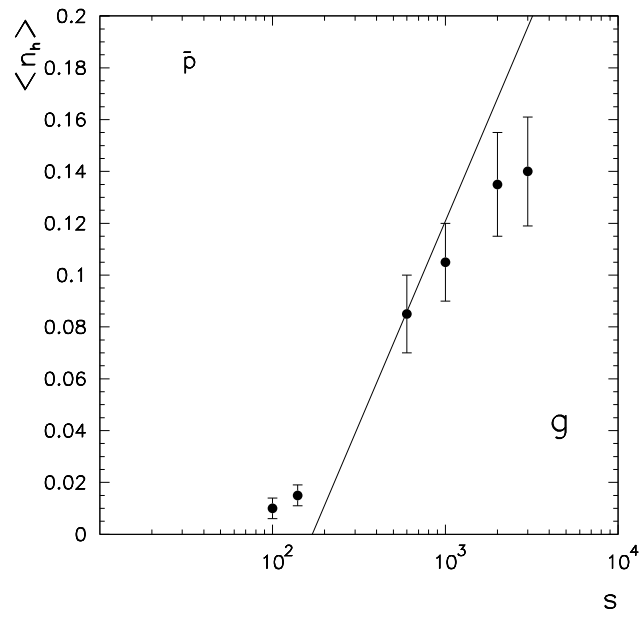
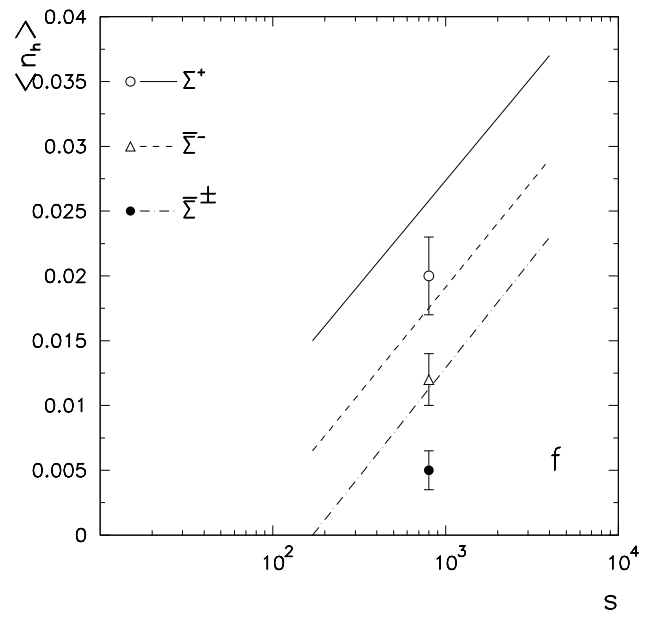
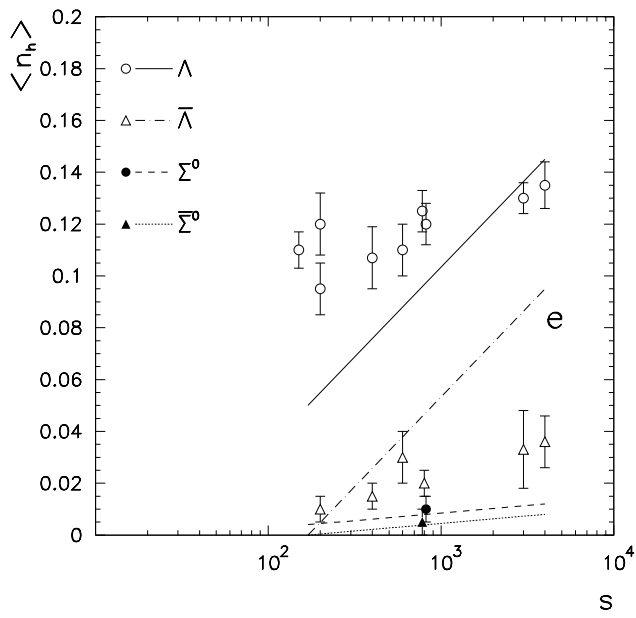


Fig.10

As an example for a quite good agreement of the predictions of quark combinatorics with the experimental data, let us consider the ratio of secondaries with total quark spins 0 and 1. In the framework of quark combinatorial calculus one assumes that in the multiparticle production process a cloud of quarks and antiquarks with non-correlated spin is formed. In such a cloud the ratio of the number of $q\bar{q}$ pairs with total quark spin $s_{q\bar{q}} = 1$ and of those with $s_{q\bar{q}} = 0$ is 3 : 1. Supposing that the mesons are formed by quarks and antiquarks independently of their spin projections, this ratio has to be also true for the produced mesons. The multiplicity of meson states with $s_{q\bar{q}} = 1$ is proportional to the multiplicity of $s_{q\bar{q}} = 0$ states as 3 : 1. In hadron-hadron collisions this relation is valid for both the fragmentational and the central regions.

The condition 3 : 1 has to be fulfilled for mesons belonging to the same $SU(6)$ multiplet. Examples for that can be the well-known relations $\rho : \pi = K^* : K = 3 : 1$ for the directly produced mesons of the lowest 36-plet. Summing over all multiplets, we obtain

$$\frac{\sum_L \langle n_{M(L;s=1)} \rangle}{\sum_L \langle n_{M(L;s=0)} \rangle} \equiv \frac{V}{P} = 3. \quad (42)$$

It is convenient to verify this relation on secondary K -mesons K , $K^*(890)$, $K^*(1420)$, since strange particles appear as decay products to a less extent than π -mesons.

Experimental data on $pp \rightarrow$ kaons (405 GeV/c, [41]) and $K^-p \rightarrow$ kaons (32 GeV/c, [42]) provide a possibility to test the condition (42). (The results of the measurements are presented in [9], Table 7.1.) The main contribution to the cross section is given by the production of the $L = 0$ multiplet. Indeed, due to the combinatorial calculus the direct production of the vector mesons is three times as large as that of the pseudoscalar mesons. Thus, the total amount of the secondary mesons with $L = 0$ is $4/3V$. The weight of tensor mesons in the $L = 1$ multiplet is $5/12$, hence $12/5T$ mesons with $L = 1$ are produced. The production of mesons with $s_{q\bar{q}} = 1$ in the multiplets with $L = 0$ and $L = 1$ is V and $9/5T$, respectively. (The value $V + \frac{9}{5}T$ which is the contribution of mesons with $s_{q\bar{q}} = 1$ in the S -wave and P -wave multiplets is also given in [9], Table 7.1.) As it is seen from the data, the experimental value is in each case around 75% of the total cross sections of kaons, in accordance with the predictions of quark combinatorics.

3 Quark combinatorics in hadronic Z^0 decays

Precision measurements [29] of hadron production in the $Z^0 \rightarrow hadron$ decay allow us to clarify some key problems of multiparticle production processes in quark induced jets. Indeed, in jets the mechanism of hadronization manifests itself explicitly, and, hence, it may be especially important to investigate multiparticle production in such processes.

Having in mind the intense experimental search for exotic meson states, it is desirable to obtain an independent verification of the basic statements of quark combinatorics. The quark combinatorial calculus is now widely used as a tool to investigate meson resonances of masses 1.0-2.5 GeV in order to determine their quark-gluon content (see, for instance, [33]-[35]). While in these investigations the qualitative picture of the cloud structure of sea quarks is not necessarily used, the notion of the "suppression parameter" for the production of strange quarks continues to play an important rôle, and it is identical to that used in multiparticle production processes.

We consider yields of vector (ρ, ω, \bar{K}^*) and pseudoscalar (π, K) mesons in hadronic Z^0 decays. There exists rich experimental information about these processes, determined by

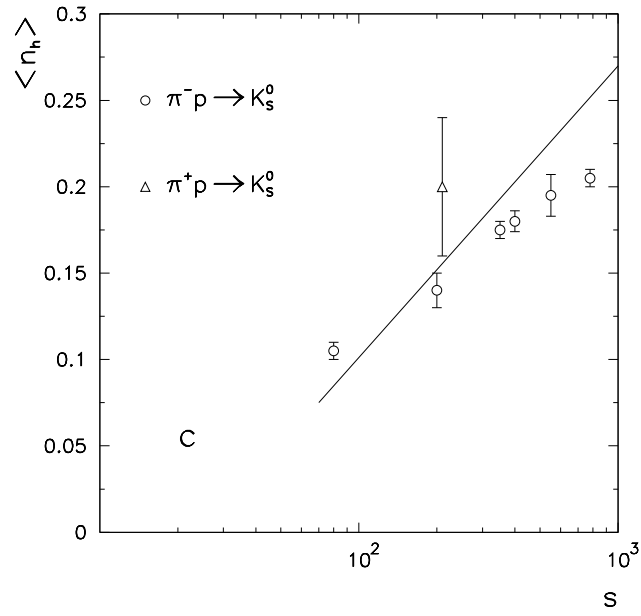
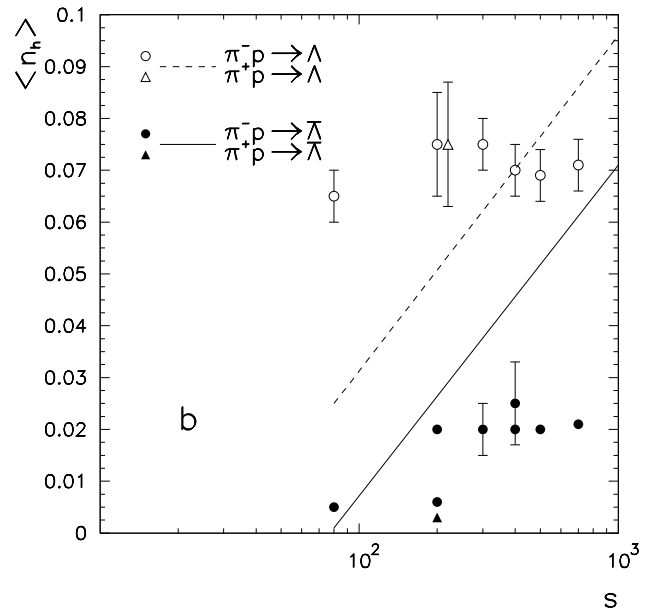
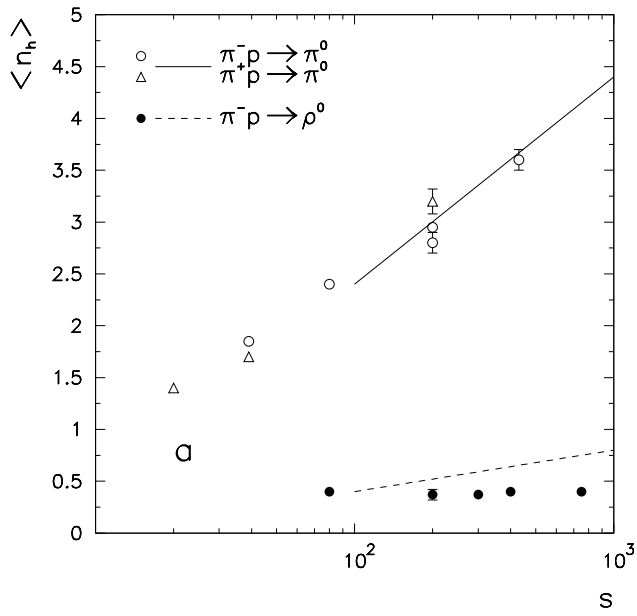


Fig.11

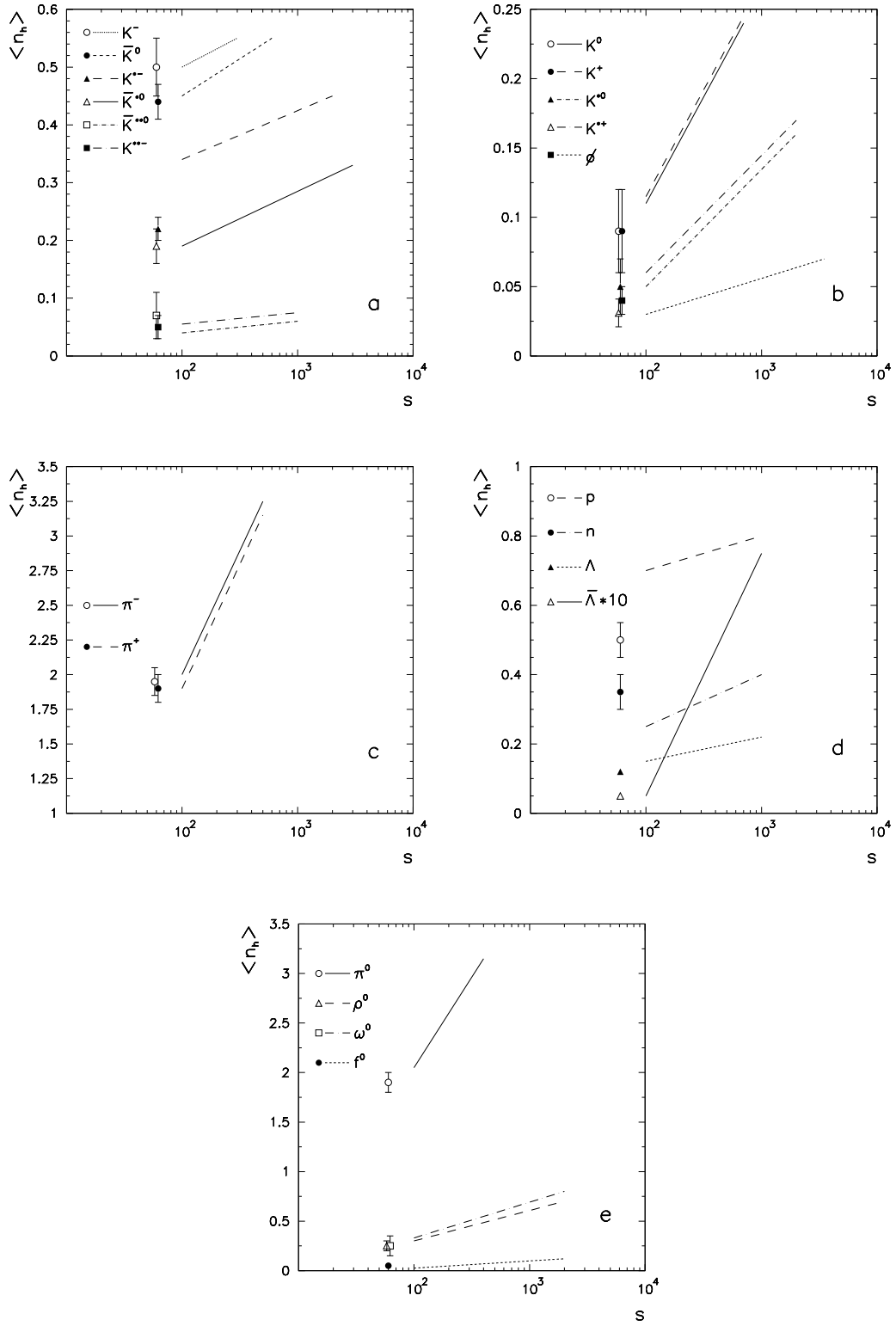


Fig.12

transitions $Z^0 \rightarrow q\bar{q} \rightarrow \text{hadrons}$. Light-flavour mesons, produced in quark jets $Z^0 \rightarrow u\bar{u}$, $Z^0 \rightarrow d\bar{d}$ and $Z^0 \rightarrow s\bar{s}$, are created with probabilities in the proportion

$$u\bar{u} : d\bar{d} : s\bar{s} = 0.26 : 0.37 : 0 : 37. \quad (43)$$

The large mass of the Z^0 boson enables us to observe in the hadronic decays $Z^0 \rightarrow q\bar{q} \rightarrow \text{hadrons}$ the characteristic features of both multiparticle production (central region of quark jets) and meson decay (fragmentation production) processes.

Data given in [29] and [53]-[55] provide spectra of vector and pseudoscalar mesons, $d\sigma/dx(Z^0 \rightarrow V + X)$ and $d\sigma/dx(Z^0 \rightarrow P + X)$, in a broad interval of x , hence, it becomes possible to compare them with the predictions of quark combinatorics [32].

As we have seen, there are two types of relations which reflect different aspects of the mechanism of multiparticle production. The first type connects secondary particles belonging to the same $SU(6)$ multiplet. These are, for example, relations between vector mesons and pseudoscalar mesons. Assuming that quarks are created arbitrarily, without colour correlation, quark combinatorics predict a production probability proportional to the spin states. In the case of vector mesons this is $V/P = 3$. These relations are valid, however, only for prompt particle production and not for particles which are decay products of higher resonances.

The second type of relations in quark combinatorics which can be investigated in the decays of Z^0 bosons into hadrons is that between secondary mesons and baryons. The hadronic decays of Z^0 bosons are determined by processes like $Z^0 \rightarrow q\bar{q} \rightarrow \text{hadrons}$. We consider decays into light hadrons; as we have seen, light quarks $u\bar{u}$, $d\bar{d}$ and $s\bar{s}$ are produced with nearly equal probabilities, there are no distinguished flavours.

3.1 Prompt production in the central region of the quark jet and the vector-pseudoscalar ratio

The prompt verification of (8) and (42) is rather difficult, since in multiparticle production processes a large number of resonances is produced; we took this into account by (29), (30). One can try to overcome the ambiguities related to the resonance production by considering all existing resonances and their decays into all possible channels. This is the scenario suggested in [46],[47]. However, there are some problems. Indeed, the number of resonances observed and cited in the compilation [48] is a comparatively small fraction of the whole set of existing states. This can be seen, e.g., from recent investigations of meson production data [49]-[51], where a large number of new meson states with masses in the region 1950-2350 MeV is reported. It is obvious that those resonances are first discovered which can be easily detected; one should also have in mind that all observed resonances have multiplet partners which are produced with approximately the same probabilities. Their decays form a background which prevents us to check directly (8) and (42). Another obstacle is the effect of accumulation of widths of overlapping resonances, which has been seen for scalar-isoscalar mesons in the region 1200-1600 MeV [51],[53]. As a result of width accumulation, a broad state ($\Gamma/2 \sim 400 \text{ MeV}$) was formed; as it was said in [52], similar states can exist in other waves, other mass regions. At the time being, it does not seem to be possible to take into account the productions and decays of such broad states. Still, the investigation of jet processes in the large x region opens a way to test the relations (8) and (42).

The decay processes increase the contribution of lighter particles, such as pions and kaons in the case of mesons, and nucleons in the case of baryons. However, in jet processes $Z^0 \rightarrow q\bar{q} \rightarrow \text{hadrons}$ considered in [29], [53]-[55], the spectra reach the maximum when the momentum x carried by the hadron is small, and they decrease rapidly when $x \rightarrow 1$. This leads to a rapid increase in the contribution of the promptly produced particles with the increase of x , since the decay products carry only a fraction of x of the initial resonance. It is just this feature which enables us to estimate the probability ratios for promptly produced hadrons.

Our analysis shows that the ratio V_{prompt}/P_{prompt} is the same for the Pomeron ladder in hadron-hadron collisions and for quark jets, despite of the different structure of the colour exchanges in these processes.

Investigations of the QCD-Pomeron [56],[57] shed light on the quark-gluon structure of the multiperipheral ladder in hadron collisions and allowed us to deal with meson yields in the central region on a new level.

When considering central production in the $Z^0 \rightarrow q\bar{q} \rightarrow \text{hadrons}$ decay, we start with the standard mechanism of soft colour neutralisation of the outgoing quarks: newly-born quark-antiquark pairs are produced in multiperipheral ladder (see Fig.13a), which provides the transfer of the colour from antiquark to quark. The discontinuity of the self-energy diagram of Fig.13b (determined by cutting through hadronic states, dashed line in Fig.13b) defines the transition cross section $Z^0 \rightarrow \text{hadrons}$, while the quark-gluon block inside the big quark loop determines the confinement forces. Similarly, the inclusive production cross section of the meson in the central region is provided by the discontinuity of the diagram of Fig.13c. The quark loop $\text{meson} \rightarrow q\bar{q} \rightarrow \text{meson}$ shown in Fig.13c with the production of vector or pseudovector mesons determines the relative probabilities of these particles. The chain of the quark loops shown in Figs.13b, 13c and 13d (below we denote this chain as A) contains both colour singlet ($c = 1$) and colour octet ($c = 8$) components: $A = A_1 + A_8$. According to the rules of $1/N$ -expansion [19], the main contribution is due to the octet component. The idea that the quark leaves the confinement trap by the production of new quark-antiquark pairs is rather old; (see, for example, [9], Sections 7 and 9, as well as [10]. Following Gribov's ideas in understanding the confinement mechanism [8], we use the jet structure shown in Fig.13a assuming that the t -channel exchange by quark is a constructive element of the jet.

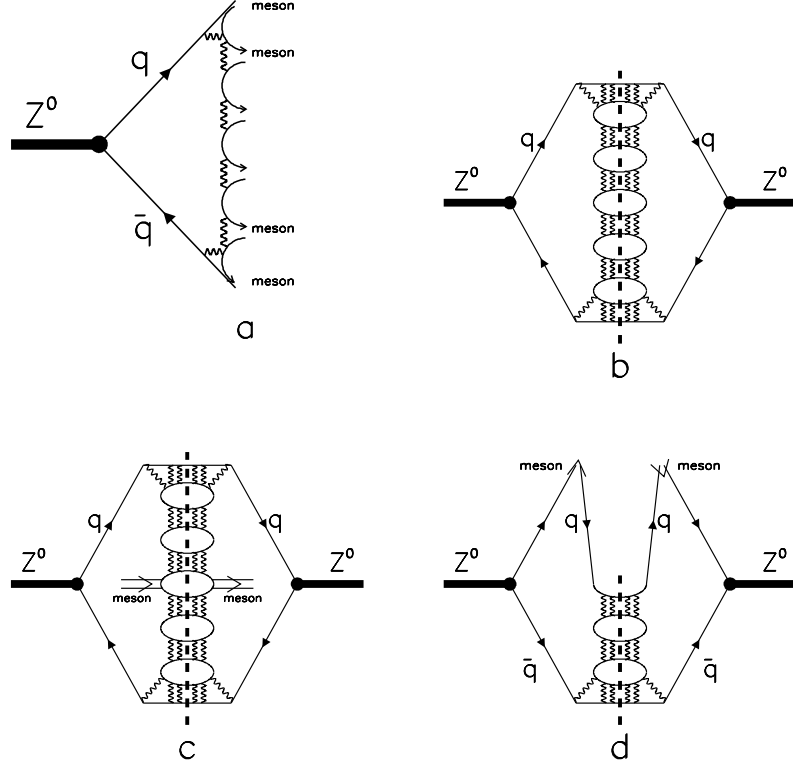


Fig.13

Spectroscopic calculations (see, for example, [60]) support the hypothesis about the scalar type of confinement forces; accordingly, we assume that the chain A realizes the t -channel exchange with $J^P = 0^+$.

The calculation of the block for central meson production proves that Eq.(42) is satisfied, if the wave functions of mesons (V and P) belonging to the same multiplet are equal.

Let us discuss the prompt production of vector and pseudoscalar mesons (for definiteness, ρ and π) in the central region of a quark jet. The production cross section is determined by the discontinuity of the diagram shown in Fig.13c; it is redrawn in Fig.14a. A specific feature of the production of ρ and π is the presence of a loop diagram, which is shown separately by Fig.14b. Below, we calculate these loop diagrams for ρ and π using the spectral integration technique which is discussed in detail in [58],[59]. Within this technique the loop diagrams are expressed in terms of the ρ and π light-cone wave functions.

But first, let us present the result of our calculations.

Direct calculations lead to the following formulae for the inclusive cross section of the ρ and π mesons at $x \sim 0$:

$$\frac{d\sigma}{dx}(Z^0 \rightarrow \rho + X) = \frac{1}{16\pi^3} \int_0^1 \frac{d\xi}{\xi(1-\xi)} \int d^2\mathbf{k}_\perp \psi_\rho^2(\xi, \mathbf{k}_\perp) \cdot 3\Pi_Z(W_1^2, W_2^2)$$

$$\frac{d\sigma}{dx}(Z^0 \rightarrow \pi + X) = \frac{1}{16\pi^3} \int_0^1 \frac{d\xi}{\xi(1-\xi)} \int d^2\mathbf{k}_\perp \psi_\pi^2(\xi, \mathbf{k}_\perp) \cdot \Pi_Z(W_1^2, W_2^2) \quad (44)$$

Here ψ_ρ and ψ_π are quark wave functions of ρ and π mesons, ξ and \mathbf{k}_\perp are quark light-cone variables (the fraction of momentum carried by a quark along the z -axis and its momentum in the (x, y) -plane, respectively). In (44) one can see explicit expressions related to the production of ρ and π mesons. The rest (contributions from the large quark loop as well as from ladder diagrams) is denoted in (44) as $\Pi_Z(W_1^2, W_2^2)$, which depends on the invariant energies squared for the quark chains, W_1^2 and W_2^2 . Multiperipheral kinematics gives

$$W_1^2 W_2^2 \simeq \xi(1-\xi)(m^2 + k_\perp^2)M_Z^2. \quad (45)$$

Here M_Z is the mass of the Z^0 boson.

The factor 3 in the ρ production cross section is the result of summation over polarizations of the vector particle.

Equation (44) demonstrates directly that, if quark wave functions of ρ and π are identical (what is assumed by the quark multiplet classification of these mesons), then at $x \sim 0$ we have $d\sigma(Z^0 \rightarrow \rho + X)/dx : d\sigma(Z^0 \rightarrow \pi + X)/dx = 3 : 1$. Let us repeat that both (44) and the diagrams of Figs.13c, 14a, 14b stand for promptly produced mesons.

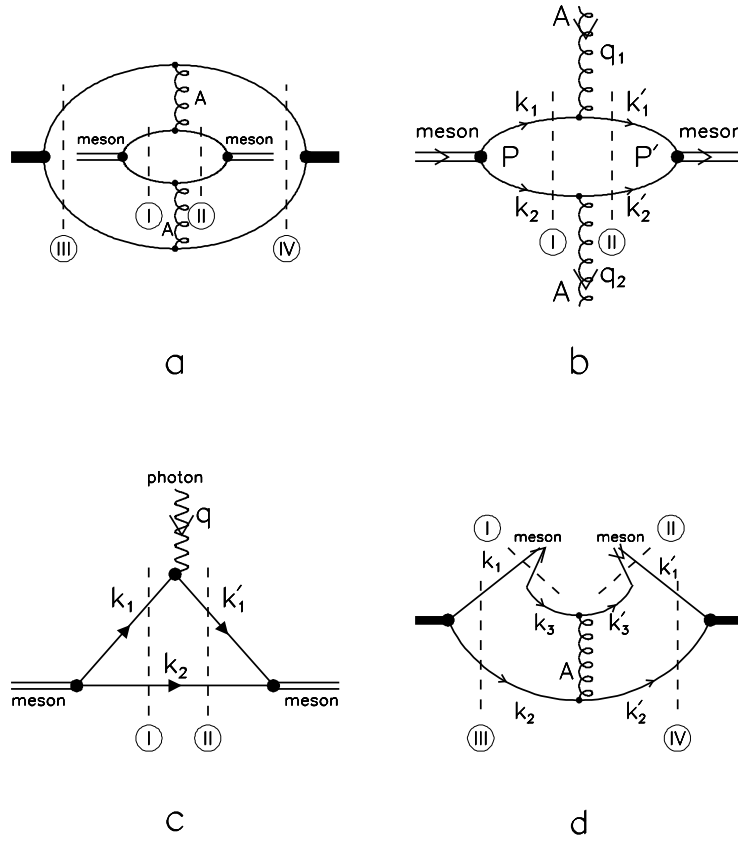


Fig.14

Let us calculate the diagram of Fig.14a in terms of a spectral integration (see also [61],[62]):

- (i) quark loops in Fig.14a are taken energy-off-shell;
- (ii) for the energy-off-shell quark loops the discontinuities are calculated (corresponding cuts are shown by the dotted lines I, II, III and IV);
- (iii) the spectral integrals are determined by the discontinuities being the integrands.

First, consider the double spectral integral which corresponds to the cuts III and IV, which are the spectral integrals over effective masses squared, M^2 and M'^2 , in the transitions $Z^0 \rightarrow q\bar{q}$ and $q\bar{q} \rightarrow Z^0$:

$$\int_{4m^2}^{\infty} \frac{dM^2 dM'^2}{\pi^2} \frac{g_Z(M^2)g_Z(M'^2)}{(M^2 - M_Z^2)(M'^2 - M_Z^2)} \times \int d\Phi(P_Z; p_1, p_2) d\Phi(P'_Z; p_3, p_4) S_Z T(p; q_1, q_2) A(W_1^2, q_1^2) A(W_2^2, q_2^2). \quad (46)$$

Here $g_Z(M^2)$ is the vertex function for the $Z^0 \rightarrow q\bar{q}$ transition and M_Z is the Z^0 boson mass. The factors $d\Phi(P_Z; p_1, p_2)$ and $d\Phi(P'_Z; p_3, p_4)$ are phase spaces related to the cuts III and IV. S_Z is the spin factor for the big quark loop in Fig.14a. The amplitudes $A(W_i^2, q_i^2)$ ($i = 1, 2$) refer to the quark-gluon chains with the t -channel scalar quantum numbers, and $T(p; q_1, q_2)$ is the block which corresponds to the small quark loop (the $q\bar{q}$ loop for

production of ρ and π mesons).

The characteristic feature of the spectral integral (46) is the large value of M_Z . Because of that one can replace, with a rather good accuracy, the poles of the spectral integrand by half-residues:

$$\frac{1}{M^2 - M_Z^2} - i\pi\delta(M^2 - M_Z^2), \frac{1}{M'^2 - M_Z^2} \rightarrow i\pi\delta(M'^2 - M_Z^2). \quad (47)$$

Equation (46) stands for the discontinuity of the amplitude which results in different signs for the half-residues in (47). Equation (47) means that the block inside of the big quark loop can be considered, with a good accuracy, as a block of the real process. This is a well-known feature of the high-energy jets; below we use it for estimating meson production amplitudes. The spectral integral (46), determined by the big quark loop, is quite common for the π and ρ production. More interesting is the spectral integral which corresponds to the amplitude $T(p; q_1, q_2)$ that is the ρ or π meson production block. This block is shown separately in Fig.14b.

The amplitude of the loop diagram of Fig.14b represented as a double dispersion integral is:

$$\begin{aligned} M &= T(p; q_1, q_2) 2p_0 (2\pi)^3 \delta^{(3)}(\mathbf{p} + \mathbf{q}_1 - \mathbf{q}_2 - \mathbf{p}'), \quad (48) \\ T(p; q_1, q_2) &= \int_{4m^2}^{\infty} \frac{ds ds'}{\pi^2} \int d\phi \frac{G_{\text{meson}}(s)}{s - \mu^2} \frac{G_{\text{meson}}(s')}{s' - \mu^2} S_{\text{meson}}. \end{aligned}$$

Here μ is the mass of produced meson, s and s' are invariant masses squared in the intermediate $q\bar{q}$ -states; G_{meson} is the vertex for the $\text{meson} \rightarrow q\bar{q}$ transition. The ratio $G_{\text{meson}}(s)/(s - \mu^2)$ determines the wave function of the produced meson up to the spin factor, and S_{meson} is the spin factor of the loop diagram Fig.14b.

In the approximation given by (47), when the jet block inside of the big quark loop is considered as a real process, one may fix $q_1 = q_2 = 0$; then the inclusive cross section is proportional to $T(p; 0, 0)$. After some calculations, the formula for $T(p; 0, 0)$ acquires a rather simple form:

$$T(p; 0, 0) = \frac{1}{16\pi^3} \int_0^1 \frac{d\xi}{\xi(1-\xi)} \int d^2k_{\perp} \left(\frac{G_{\text{meson}}(s)}{s - \mu^2} \right)^2 S_{\text{meson}}, \quad (49)$$

where $s = m_{\perp}^2 / (\xi(1 - \xi))$.

The amplitude $T(p; 0, 0)$ alone does not determine the inclusive cross section $d\sigma/dx(Z^0 \rightarrow \text{meson} + X)$ because the amplitudes $A(W_1^2, 0)$ and $A(W_2^2, 0)$ depend on ξ and k_{\perp}^2 , see (45). Taking into account this dependence, one has at $x \sim 0$:

$$\begin{aligned} \frac{d\sigma}{dx}(Z^0 \rightarrow \text{meson} + X) &\sim \\ &\frac{1}{16\pi^3} \int_0^1 \frac{d\xi}{\xi(1-\xi)} \int d^2k_{\perp} \left(\frac{G_{\text{meson}}(s)}{s - \mu^2} \right)^2 S_{\text{meson}} \Pi(W_1^2, W_2^2). \quad (50) \end{aligned}$$

The spin factor S_{meson} is closely related to the

The spin factors S_{ρ} and S_{π} at $q_1 = q_2 = 0$ are:

$$\begin{aligned} S_{\pi} &= -\text{Sp} \left(i\gamma_5 (\hat{k}_1 + m) (\hat{k}'_1 + m) i\gamma_5 (-\hat{k}'_2 + m) (-\hat{k}_2 + m) \right) \\ S_{\rho} &= -\text{Sp} \left(\gamma_{\alpha}^{\perp} (\hat{k}_1 + m) (\hat{k}'_1 + m) \gamma_{\alpha}^{\perp} (-\hat{k}'_2 + m) (-\hat{k}_2 + m) \right). \quad (51) \end{aligned}$$

We have taken into account here that the quark–gluon ladder carries quantum numbers of the scalar state, $J^P = 0^+$; hence the quark-ladder vertex is unity. The ρ -meson vertex is:

$$\gamma_\alpha^\perp = g_{\alpha\alpha'}^\perp \gamma_{\alpha'} , \quad g_{\alpha\alpha'}^\perp = g_{\alpha\alpha'} - \frac{P_\alpha P_{\alpha'}}{P^2} . \quad (52)$$

In the spin factor S_ρ the summation is performed over polarizations of the meson. For the spin factors we have:

$$S_\pi = 8m^2 s , \quad S_\rho = 16 m^2 (s + 2m^2) . \quad (53)$$

Let us now demonstrate that similar spin factors determine the normalization of wave functions of the ρ -meson and the pion.

In the framework of the light-cone technique it is reasonable to introduce the wave function of a particle and its normalization using the form factor of the particle. The procedure of definition of the wave function is discussed in detail in [58],[59]. Schematically, for the $q\bar{q}$ state this procedure looks as follows.

The form factor of a composite system (for definiteness, we consider the pion form factor) is determined by the triangle diagram Fig.14c, where the photon interacts with the composite system. The form factor is represented as a double spectral integral over masses of the incoming and outgoing pion; corresponding cuttings are shown by the dashed lines I and II in Fig.14c. The structure of the amplitude of the triangle diagram for the pion has the following form:

$$A_\nu^{(tr)} = (p_\nu + p'_\nu) F_\pi(q^2) , \quad (54)$$

where p and p' are momenta of the incoming and outgoing pions, the index ν refers to the photon polarization and $F_\pi(q^2)$ is the pion form factor which, in terms of the double spectral representation, can be written as

$$F_\pi(q^2) = \int_{4m^2}^{\infty} \frac{ds ds'}{\pi^2} \int d\Phi^{(tr)}(k_1, k'_1, k_2) \frac{G_\pi(s)}{s - \mu^2} T_\pi(s, s', q^2) . \quad (55)$$

At $q^2 = 0$ one has $F_\pi(0) = 1$. Direct calculations of equation (55) in the limit $q^2 \rightarrow 0$ give:

$$1 = \int_{4m^2}^{\infty} \frac{ds}{\pi} \left(\frac{G_\pi(s)}{s - \mu^2} \right)^2 \rho(s) S_\pi^{(wf)}(s) . \quad (56)$$

Here $\rho(s)$ is the phase volume of the $q\bar{q}$ system and $S_\pi^{(wf)}(s)$ is the trace of the quark loop diagram for the pion. Using light-cone variables we come to the following form of (56):

$$1 = \frac{1}{16\pi^3} \int_0^1 \frac{d\xi}{\xi(1-\xi)} \int d^2\mathbf{k}_\perp \left(\frac{G_\pi(s)}{s - \mu^2} \right)^2 2s , \quad (57)$$

where $s = (m^2 + k_\perp^2)/(\xi(1-\xi))$. This equation enables us to introduce the pion wave function in the form

$$\psi_\pi(\xi, \mathbf{k}_\perp) = \frac{G_\pi(s)}{s - \mu^2} \sqrt{2s} , \quad (58)$$

which is normalized by the standard requirement.

Likewise, we introduce the ρ -meson wave function: it is defined by the form factor which is the spin matrix $F_{\alpha\alpha'}(q^2)$. In problems that do not deal with polarization properties of the vector particle, it is convenient to work with the trace of the form factor matrix, $\sum_{\alpha} F_{\alpha\alpha}(q^2)$, which is normalized by

$$\sum_{\alpha=1,2,3} F_{\alpha\alpha}(0) = 3. \quad (59)$$

The trace $\sum_{\alpha} F_{\alpha\alpha}(q^2)$ is determined by the expression analogous to (55), with evident substitutions $G_{\pi} \rightarrow G_{\rho}$ and $T_{\pi} \rightarrow T_{\rho}$. As a result, we obtain the normalization for the averaged form factor:

$$1 = \frac{1}{3} \sum_{\alpha=1,2,3} F_{\alpha\alpha}(0) = \int_{4m^2}^{\infty} \frac{ds}{\pi} \left(\frac{g_{\rho}(s)}{s - \mu^2} \right)^2 \rho(s) S_{\rho}^{(wf)}(s) \quad (60)$$

where

$$S_{\rho}^{(wf)}(s) = -\frac{1}{3} \text{Sp} \left[\left(\gamma_{\alpha} - P_{\alpha} \frac{\hat{P}}{P^2} \right) (\hat{k}_1 + m) \left(\gamma_{\alpha} - P_{\alpha} \frac{\hat{P}}{P^2} \right) (-\hat{k}_2 + m) \right]. \quad (61)$$

The $\rho \rightarrow q\bar{q}$ vertex, $\gamma_{\alpha} - P_{\alpha} \hat{P}/P^2$, selects three degrees of freedom of the ρ -meson. We have :

$$S_{\rho}^{(wf)}(s) = \frac{4}{3}(s + 2m^2). \quad (62)$$

In the infinite momentum frame, (60) is re-written as

$$1 = \frac{1}{16\pi^3} \int_0^1 \frac{d\xi}{\xi(1-\xi)} \int d^2\mathbf{k}_{\perp} \psi_{\rho}^2(\xi, \mathbf{k}_{\perp}), \quad (63)$$

where

$$\psi_{\rho}(\xi, \mathbf{k}_{\perp}) = \frac{G_{\rho}(s)}{s - \mu^2} \sqrt{\frac{4}{3}(s + 2m^2)}. \quad (64)$$

The normalization conditions for pion and ρ -meson wave functions define unambiguously the ratio of yields for prompt production: $\rho/\pi = 3$, if the wave functions of these mesons are similar. Indeed, the expression (50) represented in terms of wave functions ψ_{ρ} and ψ_{π} gives us (44) immediately.

We have not taken into account explicitly the colour degrees of freedom in the derivation. This, however, can be easily done. For the $meson \rightarrow q\bar{q}$ vertex the colour operator is equal to $I/\sqrt{N_c}$, where I is a unity matrix in colour space. We have two colour amplitudes, singlet and octet, for the chain of the quark loop diagrams, A_1 and A_8 . The couplings of the amplitudes A_1 and A_8 to quarks ($g(A_1)$ and $g(A_8)$) are proportional to I and λ (Gell-Mann matrices). All colour operators are the same for both pion and ρ -meson production. Because of that, the colour factors are not important for the ratio ρ/π – they are identical and cancel in the production ratio.

As was stated above, the main contribution into inclusive meson production comes from the ladder diagram A_8 . This is due to the fact that the coupling constant for the amplitude with $c = 8$ is larger than for $c = 1$. In terms of $1/N_c$ expansion $g(A_1)/g(A_8) \sim 1/\sqrt{N_c}$.

3.2 Inclusive production of mesons in the fragmentation region

The equality (42) is valid for prompt meson production, while the decays of highly excited states violate this ratio, as is seen in the experiment, providing the increase of the rate of light mesons due to resonance decay. As to ρ/π and K^*/K , the decays increase the contribution of pseudoscalar component. According to [29], $\rho^0/\pi^0 = 0.15 \pm 0.03$, and $K^*/K = 0.40 \pm 0.06$. This indicates a large contribution into spectra from the decays of highly excited states.

One should stress that the ratios V/P for beauty and charmed mesons are saturated in the fragmentation region due to the transitions $Z^0 \rightarrow b\bar{b}$ and $Z^0 \rightarrow c\bar{c}$. Therefore, in Section 3.2 we re-analyse quark combinatorics for the fragmentation region of the hadronic Z^0 decay.

The problem of the production and decay of highly excited states in hadron–hadron collisions had been discussed in [61]. The conclusion was similar: average multiplicities of the produced light mesons and baryons result mainly from the cascade decays of the highly excited resonances.

The existence of the decay of highly excited resonances is a reality that one should take into account in the verification of quark combinatorial rules. We discuss several ways of solving this problem.

One way is to check quark combinatorics for heavy particle yields, where the cascade multiplication is suppressed. An ideal example could be the production of mesons containing a b -quark. In fact, for the beauty mesons the ratio B^*/B observed in the experiment agrees with (42). When the lowest S -wave multiplet dominates in the production of heavy mesons, then one has (provided the equation (42) is fulfilled): $B \simeq B_{prompt} + B_{prompt}^* = 4B_{prompt}$, and the ratio of vector and pseudoscalar mesons is $B^*/B \simeq 0.75$.

In experiments on Z^0 decay it was observed: $B^*/B = 0.771 \pm 0.075$ [62], 0.72 ± 0.06 [62], 0.76 ± 0.10 [64], 0.76 ± 0.09 [66]; the mean value is 0.75 ± 0.04 .

For charmed mesons $D^*/D = 0.60 \pm 0.05$ [66], 0.62 ± 0.03 [67], 0.57 ± 0.05 [68]. The mean value is 0.61 ± 0.03 , which means a rise of the contribution from the decay of the non- S -wave multiplets.

The production cross section of mesons in the fragmentation region is determined by the discontinuity of the diagram of Fig.13c (the cutting of ladder diagram is shown by dashed line). Direct calculations demonstrate that (42) is satisfied with a rather good accuracy for the fragmentation region as well, provided the wave functions of vector and pseudoscalar mesons are equal.

Investigations of meson production in the fragmentation region open the way to test the rules of quark combinatorics for light–flavour hadrons, and to verify (42) in particular. As is said above, in the spectra of light–flavour hadrons the contribution of the component related to the decay of highly excited states dominates. Still, in the case of jet processes this component dominates in the central region, at $x \sim 0$, but not in the fragmentation one. The hadronic spectra for jets are maximal at $x \sim 0$, and they decrease rapidly with the growth of x . As a result, the component which comes from a resonance decay decreases quickly, because the decay products share the value $x_{resonance}$, thus entering the region of smaller x . In due course this effects a fast growth of relative contributions from prompt particle production. Therefore, the measurements of particle yields at $x \sim 0.5 - 1.0$ provide an opportunity for model–independent testing of quark combinatorics.

The inclusive production cross section of mesons in the fragmentation region is de-

terminated by the discontinuity of the diagram of Fig.14d. The spectral representation for this diagram is written as an integral over the masses of initial and final $q\bar{q}$ states in the transitions $Z^0 \rightarrow q\bar{q}$ and $q\bar{q} \rightarrow Z^0$ and over $q\bar{q}$ masses in the transitions $q\bar{q} \rightarrow meson$ and $meson \rightarrow q\bar{q}$. The amplitude of the diagram of Fig.14d reads:

$$\int_{4m^2}^{\infty} \frac{dM^2 dM'^2}{\pi^2} \frac{g_Z(M^2)g_Z(M'^2)}{(M^2 - M_Z^2)(M'^2 - M_Z^2)} \int_{4m^2}^{\infty} \frac{ds ds'}{\pi^2} \psi_{meson}(s)\psi_{meson}(s')$$

$$\times d\phi_3(k_1, k_2, k_3) d\phi_3(k'_1, k'_2, k'_3) A(W^2, (k_2 - k'_2)^2) \frac{S_{meson}^{(fr)}}{\sqrt{S_{meson}^{(wf)}(s)S_{meson}^{(wf)}(s')}}. \quad (65)$$

The vertices $g_Z(M^2)$ and $g_Z(M'^2)$ are written for the $Z^0 \rightarrow q\bar{q}$ and $q\bar{q} \rightarrow Z^0$ transitions. Spectral integrals over s and s' stand for $q\bar{q} \rightarrow meson$ and $meson \rightarrow q\bar{q}$ (where *meson* means π, ρ). The wave function ψ_{meson} of the produced meson was introduced in an explicit form in Section 3.1 for the pion and the ρ -meson, and the factors $d\phi_3(k_1, k_2, k_3)$ and $d\phi_3(k'_1, k'_2, k'_3)$ define the integration over phase spaces in the left- and right-hand parts of the diagram of Fig.14d:

$$d\phi_3(k_1, k_2, k_3) = \frac{1}{2} \frac{d^3 k_1}{(2\pi)^3 2k_{10}} \frac{d^3 k_2}{(2\pi)^3 2k_{20}}$$

$$\times (2\pi)^4 \delta^{(4)}(\tilde{P} - k_1 - k_2) \frac{1}{2} \frac{d^3 k_3}{(2\pi)^3 2k_{30}} (2\pi)^4 \delta^{(4)}(P - k_1 - k_3). \quad (66)$$

Here $\tilde{P}^2 = M^2$ and $P^2 = s$.

The block $A(W^2, (k_2 - k'_2)^2)$ defines the multiperipheral ladder (wavy line in Fig.14d). This block depends on the momentum transfer squared $(k_2 - k'_2)^2$ and the total energy squared W^2 :

$$W^2 \simeq M_Z^2(1 - x); \quad (67)$$

x is the momentum fraction carried by the produced meson: $x = 2p/M_z$, where p is the longitudinal component of meson momentum, $p_{meson} = (p + \mu_{\perp}^2/2p, 0, p)$.

The spectra $d\sigma(Z^0 \rightarrow meson + X)/dx$ fall rapidly with increasing x : this decrease is governed by $A(W^2, (k_2 - k'_2)^2)$.

All the characteristics of (65) listed above are the same for both pion and ρ -meson production, the wave functions ψ_{π} and ψ_{ρ} are also supposed to be the same. The difference may be contained in the spin factors $S_{\pi}^{(fr)}$ and $S_{\rho}^{(fr)}$ which are

$$S_{\pi}^{(fr)} = (-)\text{Sp} \left[\gamma_{\nu}^{\perp} (1 + R\gamma_5) (\hat{k}'_1 + m) i\gamma_5 (\hat{k}'_3 + m) (\hat{k}_3 + m) \right.$$

$$\times \left. i\gamma_5 (\hat{k}_1 + m) \gamma_{\nu}^{\perp} (1 + R\gamma_5) (-\hat{k}_2 + m) (-\hat{k}'_2 + m) \right];$$

$$S_{\rho}^{(fr)} = (-)\text{Sp} \left[\gamma_{\nu}^{\perp} (1 + R\gamma_5) (\hat{k}'_1 + m) \gamma_{\alpha}^{\perp} (\hat{k}'_3 + m) (\hat{k}_3 + m) \right.$$

$$\times \left. \gamma_{\alpha}^{\perp} (\hat{k}_1 + m) \gamma_{\nu}^{\perp} (1 + R\gamma_5) (-\hat{k}_2 + m) (-\hat{k}'_2 + m) \right]. \quad (68)$$

Here R is determined by the ratio g_A/g_V and the factor $\gamma_{\nu}^{\perp} (1 + R\gamma_5)$ is related to the vertex $Z^0 \rightarrow q\bar{q}$ which is determined by the vector and axial-vector interactions (the ratio of coupling constants is ~ 2.63 for the u quark and ~ 1.43 for the d quark).

After some calculations (for details see [32]) we get for the light mesons

$$\frac{S_{\pi}^{(fr)}}{S_{\pi}^{(wf)}} \simeq 2M_Z^2(1 + R^2) , \quad \frac{S_{\rho}^{(fr)}}{S_{\rho}^{(wf)}} \simeq 6M_Z^2(1 + R^2) , \quad (69)$$

which gives the ratio of the prompt yields $\rho : \pi = 3 : 1$ in the fragmentation region $x \sim 0.5 - 1$ (more generally, $V : P = 3 : 1$ for hadronic decays $Z^0 \rightarrow q\bar{q}$ with $q = u, d, s$). The same ratio appears for the production of heavy quarks $Z^0 = Q\bar{Q}$, where $Q = c, b$. For example, in the case of b quark the spin factors are:

$$\begin{aligned} \frac{S_B^{(fr)}}{S_B^{(wf)}} &\simeq 2 \left[M_Z^2 + 2m_b^2 + R^2(M_Z^2 - 4m_b^2) \right] , \\ \frac{S_{B^*}^{(fr)}}{S_{B^*}^{(wf)}} &= 6 \left[M_Z^2 + 2m_b^2 + R^2(M_Z^2 - 4m_b^2) \right] , \end{aligned} \quad (70)$$

and thus the ratio $B_{prompt}^* : B_{prompt}$ also equals 3.

We have seen that $V/P = 3$ in the fragmentation region as well as in the central region. However, in the central region the comparison of quark combinatorics with experiment is hampered by the presence of a number of the decay products of highly excited resonances, while in the fragmentation region this contribution is suppressed by rapidly decreasing spectra. This means that the fragmentation region allows us to perform a model-independent verification of quark combinatorics. We compare the calculated ratio with ALEPH data [29]. For meson spectra at $x \sim 0.2 - 0.8$ we have fitted the spectra $(1/\sigma_{tot})d\sigma/dx$ to the sum of exponents $\sum C_i e^{-b_i x}$; the calculation results are presented in Fig.15 for π^{\pm}, π^0, ρ^0 and (p, \bar{p}) . The ratio of fitting curves drawn with calculation errors (shaded area) is shown in Fig.16a for ρ/π . We see that for $0.6 < x < 0.8$ the data are in reasonable agreement with the prediction $\rho/\pi = 3$. Figures 16b,c demonstrate the ratios K^{*0}/K^0 and $K^{*\pm}/K^{\pm}$: the data do not contradict the prediction, though the errors are too large to conclude anything more definite.

3.3 Suppression of the strange and heavy quark productions

In hadronic multiparticle production processes (in jet processes of the type of $Z^0 \rightarrow \text{hadrons}$ or in hadron-hadron collisions at high energies) the production of strange quarks is suppressed. Strong suppression is observed for the production of heavy quarks $Q = c, b$. One can assume that this suppression, being of the same nature for different reactions, is related to the mechanism of the production of new quarks at large separations of colour objects. This mechanism is seen in its pure form in the two-particle decays (the corresponding diagram is shown in Fig.17a). The block of the production of a new $q\bar{q}$ pair in the two-particle decay is the same as that of meson production in jet processes (Fig.17b), so it is reasonable to suppose that the suppression mechanism of the production of new quarks is similar for these processes.

The decay of the $q\bar{q}$ state takes place as follows: the quarks of the excited state leave the region where they were kept by the confinement barrier, and at a sufficiently large separation a new quark-antiquark pair will be produced inevitably: together with the incident quarks, these new quarks then form mesons (i.e. free particles). Schematically, this process (which is the leading one in terms of the $1/N$ expansion) is shown on the diagram of Fig.17a: two quarks fly away (with the momenta p_1 and p_2), and at large quark separations the gluonic field produces a new $q\bar{q}$ pair (the quarks with momenta k_2, k_3); then the primary quark (now with momentum k_1) joins the newly-born one (k_2) creating a meson. Similarly, another newly-born quark (k_3) joins the other primary quark (now with momentum k_4) producing the second meson.

The block with the quark-antiquark production, that is the transition

$$q(p_1) + \bar{q}(p_2) \rightarrow q(k_1) + \bar{q}(k_2) + q(k_3) + \bar{q}(k_4) \quad (71)$$

is the key process that determines the decay physics; it is shown separately in Fig.17c. The process (71) is responsible for the fact that quarks leave the confinement trap. For modeling this, quark combinatorics uses the hypothesis of soft hadronization. It suggests that in the ladder of produced quarks (Figs.13a, 17c) the contribution comes from small momentum transfers (of the order of $R_{confinement}^{-2}$). In the framework of the space-time picture this means that new $q\bar{q}$ pairs are produced at large separations, when colour objects leave the confinement well.

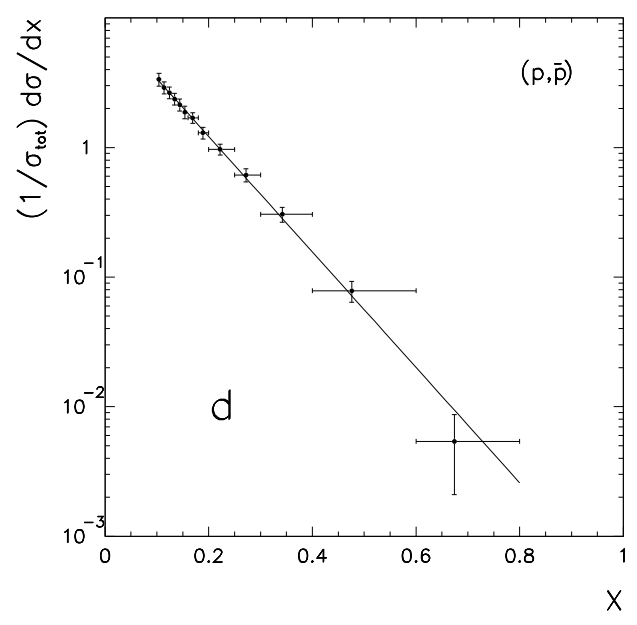
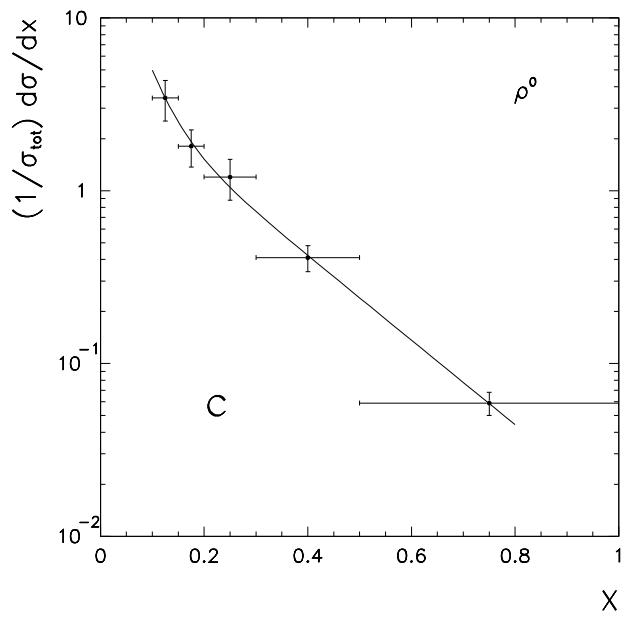
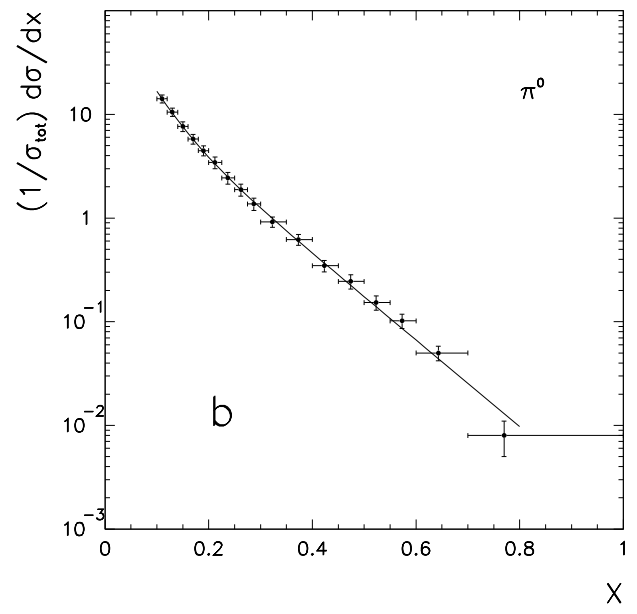
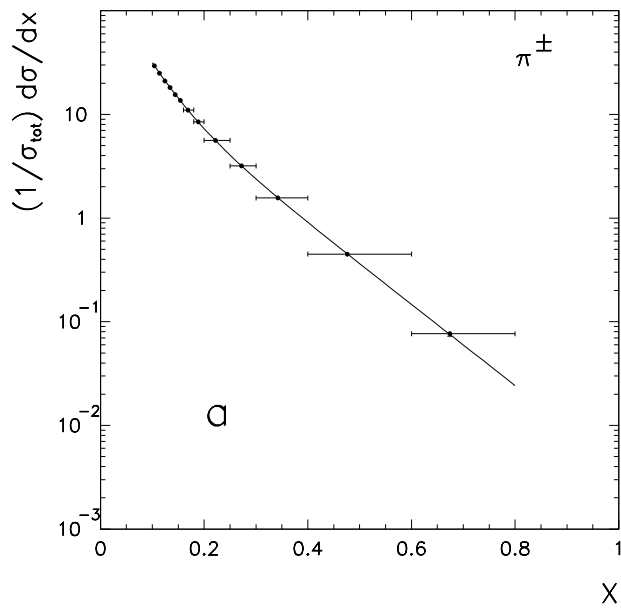


Fig.15

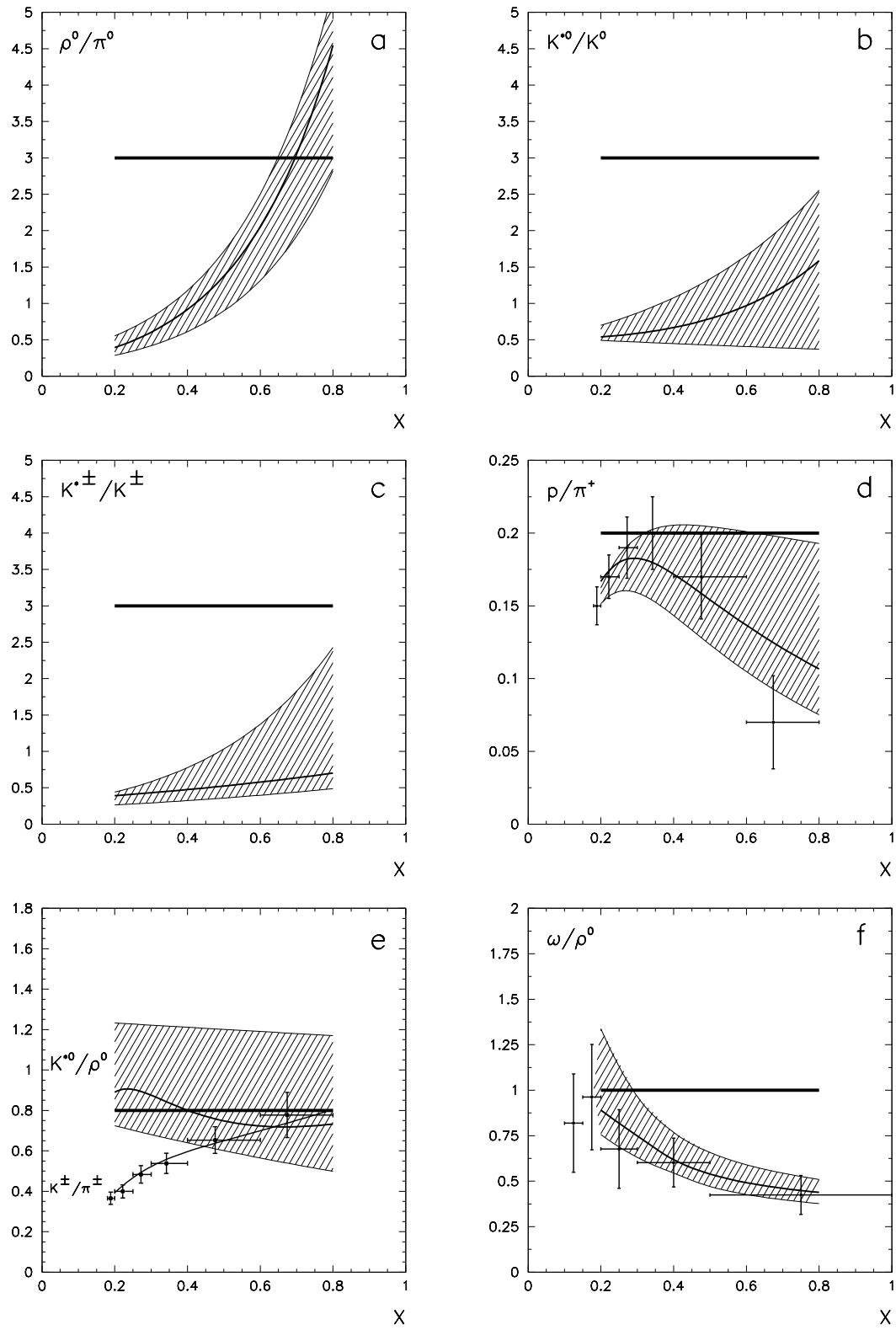


Fig.16

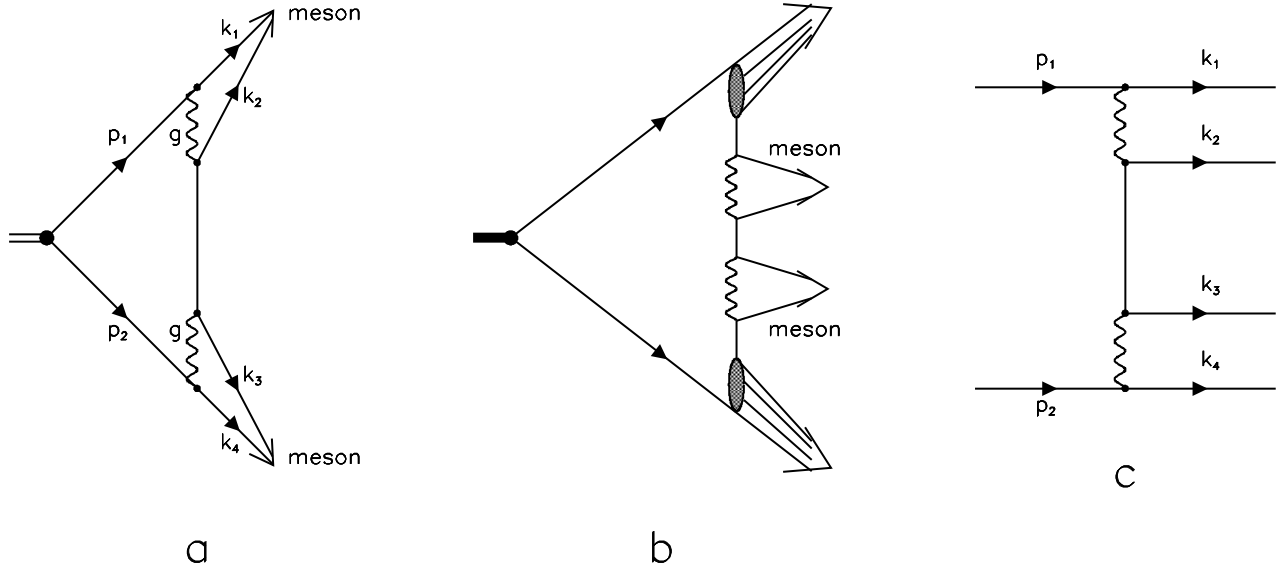


Fig.17

The soft hadronization hypothesis applied to the decay processes treats the ladder diagram of Fig.17c for the decay amplitude of Fig.17a in the same way as for jet production, Fig.17b: process (71) is an elementary subprocess both for the high-energy ladder and the two-particle decay amplitude, and the momentum transfers which enter the amplitude (71) appear to be small in the hadronic scale, $\sim R_{confinement}^{-2}$.

Let us consider in detail the decay amplitude of Fig.17a, performing calculations, as before, in the framework of the spectral representation with the light-cone wave functions for $q\bar{q}$ states.

By using the notations

$$\begin{aligned}
 P &= p_1 + p_2, & k_{12} &= k_1 + k_2, & k_{34} &= k_3 + k_4, \\
 M^2 &= (k_1 + k_2)^2, & s_{12} &= (k_1 + k_2)^2, & s_{34} &= (k_3 + k_4)^2
 \end{aligned}
 \tag{72}$$

we have the following spectral representation for the amplitude:

$$\begin{aligned}
 A(q\bar{q} \text{ state} \rightarrow \text{two mesons}) &= \int_{4m^2}^{\infty} \frac{dM^2}{\pi} \Psi_{in}(M^2) d\Phi(P; p_1, p_2) \int_{(m+m_s)^2}^{\infty} \frac{ds_{12} ds_{34}}{\pi^2} \\
 &\times t(p_1, p_2; k_1, k_2, k_3, k_4) d\Phi(k_{12}; k_1, k_2) d\Phi(k_{34}; k_3, k_4) \Psi_1(s_{12}) \Psi_2(s_{34}) .
 \end{aligned}
 \tag{73}$$

Here the masses of newly-born quarks $i = 2, 3$ are denoted as m_s , thus opening the way to consider the decay with strange quark production. The transition amplitude (71) of Fig. 17c is denoted as $t(p_1, p_2; k_1, k_2, k_3, k_4)$. The decay amplitude (72) is written in terms of meson wave functions: for the initial state it is $\Psi_{in}(M^2)$, and for outgoing mesons they are $\Psi_1(s_{12})$ and $\Psi_2(s_{34})$.

Thus, the decay amplitude A is a convolution of the transition amplitude (71) with wave functions of initial and outgoing mesons:

$$A(q\bar{q} \text{ state} \rightarrow \text{two mesons}) = \Psi_{in} \otimes t \otimes \Psi_1 \Psi_2 .
 \tag{74}$$

Let us turn to the principal point, namely: the evaluation of the region in momentum space selected by the transition amplitude of Fig.17c within the assumption of soft hadronization.

The hypothesis of soft hadronization means that the ladder diagram of Fig.17c has a peripheral structure: it requires the momentum transfers to the $q\bar{q}$ block to be small, of the order of $1/R_{confinement}^2$. So

$$\begin{aligned} -(p_1 - k_1)^2 &\simeq (\mathbf{p}_{1\perp} - \mathbf{k}_{1\perp})^2 \sim R_{confinement}^{-2}, \\ -(p_2 - k_4)^2 &\simeq (\mathbf{p}_{2\perp} - \mathbf{k}_{4\perp})^2 \sim R_{confinement}^{-2}. \end{aligned} \quad (75)$$

Likewise, the momentum transfer squared in the quark propagator (see Fig.17c) is of the order

$$(p_1 - k_1 - k_2)^2 \simeq -(\mathbf{p}_{1\perp} - \mathbf{k}_{1\perp} - \mathbf{k}_{2\perp})^2. \quad (76)$$

In the simplest approximation, taking into account only the t -channel propagators, we can write the formula for $t(p_1, p_2; k_1, k_2, k_3, k_4)$ in the form

$$\begin{aligned} t(p_1, p_2; k_1, k_2, k_3, k_4) &= \frac{g}{m_g^2 + (\mathbf{p}_{1\perp} - \mathbf{k}_{1\perp})^2} \\ &\times \frac{g^2 (m_s - \gamma(\mathbf{p}_{1\perp} - \mathbf{k}_{1\perp} - \mathbf{k}_{2\perp}))}{m_s^2 + (\mathbf{p}_{1\perp} - \mathbf{k}_{1\perp} - \mathbf{k}_{2\perp})^2} \cdot \frac{g}{m_g^2 + (\mathbf{p}_{2\perp} - \mathbf{k}_{4\perp})^2}, \end{aligned} \quad (77)$$

where γ is the Dirac matrix. To avoid ultrared divergence, the effective mass of the soft gluon is introduced into the gluon propagator (see, for example, [69]).

The equation (77) does not state that the transition amplitude $t(p_1, p_2; k_1, k_2, k_3, k_4)$ selects large distances. At this point the amplitude (77) may be, however, improved by incorporating form factors into the gluon emission vertex:

$$g \rightarrow g((\mathbf{p}_{1\perp} - \mathbf{k}_{1\perp})^2), \quad g \rightarrow g((\mathbf{p}_{2\perp} - \mathbf{k}_{4\perp})^2). \quad (78)$$

With equations (77) and (78) the amplitude A reads:

$$\begin{aligned} A(q\bar{q} \rightarrow \text{two mesons}) &= \int_0^1 \frac{dx_1 dx_2 \delta(1 - x_1 - x_2)}{16\pi^2 x_1 x_2} \int d\mathbf{p}_{1\perp} d\mathbf{p}_{2\perp} \delta(\mathbf{p}_{1\perp} + \mathbf{p}_{1\perp}) \\ &\times \int_{y_1 \gg y_2} \frac{dy_1 dy_2 \delta(1 - y_1 - y_2)}{16\pi^2 y_1 y_2} \cdot \int d\mathbf{k}_{1\perp} d\mathbf{k}_{2\perp} \delta(\mathbf{k}_{1\perp} + \mathbf{k}_{2\perp}) \\ &\times \int_{y_4 \gg y_3} \frac{dy_3 dy_4 \delta(1 - y_3 - y_4)}{16\pi^2 y_3 y_4} \int d\mathbf{k}_{3\perp} d\mathbf{k}_{4\perp} \delta(\mathbf{k}_{3\perp} + \mathbf{k}_{4\perp}) \Psi_{in}(x_1, x_2; \mathbf{p}_{1\perp}, \mathbf{p}_{2\perp}) \\ &\times \frac{g((\mathbf{p}_{1\perp} - \mathbf{k}_{1\perp})^2)}{m_g^2 - (\mathbf{p}_{1\perp} - \mathbf{k}_{1\perp})^2} \frac{g^2 (m_s - \gamma(\mathbf{p}_{1\perp} - \mathbf{k}_{1\perp} - \mathbf{k}_{2\perp}))}{m_s^2 + (\mathbf{p}_{1\perp} - \mathbf{k}_{1\perp} - \mathbf{k}_{2\perp})^2} \frac{g((\mathbf{p}_{2\perp} - \mathbf{k}_{4\perp})^2)}{m_g^2 + (\mathbf{p}_{2\perp} - \mathbf{k}_{4\perp})^2} \\ &\times \Psi_1(y_1, y_2; \mathbf{k}_{1\perp}, \mathbf{k}_{2\perp}) \Psi_2(y_3, y_4; \mathbf{k}_{3\perp}, \mathbf{k}_{4\perp}). \end{aligned} \quad (79)$$

This is the expression for the decay amplitude which makes it possible to discuss the rules of quark combinatorics.

In a rough approximation that still gives a qualitatively correct answer, we neglect the momenta in the propagator of newly-born quarks:

$$\frac{g^2 (m_s - \gamma(\mathbf{p}_{1\perp} - \mathbf{k}_{1\perp} - \mathbf{k}_{2\perp}))}{m_s^2 + (\mathbf{p}_{1\perp} - \mathbf{k}_{1\perp} - \mathbf{k}_{2\perp})^2} \rightarrow \frac{g^2}{m_s}. \quad (80)$$

We have

$$A(q\bar{q} \text{ state} \rightarrow \text{two mesons}) = \frac{\alpha_s}{m_s} \cdot (\Psi_{in} \otimes t \otimes \Psi_1 \Psi_2) , \quad (81)$$

This equation tells us that the probability to produce non-strange and strange quarks, $u\bar{u} : d\bar{d} : s\bar{s} = 1 : 1 : \lambda$, is determined by the ratio of masses squared of non-strange (u, d) to strange (s) quark. Introducing the constituent quark masses in the soft region, $m_u \simeq m_d \equiv m = 350$ MeV and $m_s \simeq 500$ MeV, we get:

$$\lambda \simeq \frac{m^2}{m_s^2} \simeq 0.5. \quad (82)$$

The equations (80) and (81) justify the statements of quark combinatorics applied to the decay processes [9],[70]-[72]. Of course, here we suppose that meson wave functions belonging to the same multiplet are identical.

Equation (82) gives us just a rough evaluation for λ , for in (80) we neglected momentum transfers squared compatible with light quark masses. In more sophisticated evaluations of λ , one may take into account the momentum dependence of the quark propagator:

$$\frac{1}{m_s^2 + (\mathbf{p}_{1\perp} - \mathbf{k}_{1\perp} - \mathbf{k}_{2\perp})^2} \rightarrow \frac{1}{m_s^2 + \langle k^2 \rangle}, \quad (83)$$

where $\langle k^2 \rangle$ is a typical momentum squared inherent to the considered decay process. Therefore,

$$\lambda = \frac{m^2 + \langle k^2 \rangle}{m_s^2 + \langle k^2 \rangle}. \quad (84)$$

For standard decays of light resonances $\langle k^2 \rangle \sim 0.1 - 0.3$ (GeV/c)², and this results in the increase of λ compared to (82). Indeed, in the analysis [72] $\lambda \sim 0.7$ was found. Actually, (84) demonstrates that λ can vary depending on different types of reactions.

Let us now turn to the processes of the $q\bar{q}$ pair production in jet processes $Z^0 \rightarrow q\bar{q} \rightarrow \text{hadrons}$, which is shown in Fig.17b. All the above considerations, which have been used for the decay of a resonance into two mesons, can be applied to this process. As a result, we obtain the following formula which is a counterpart of (81):

$$A(Z^0 \rightarrow \text{two mesons} + X) = \frac{\alpha_s}{m_s} \cdot (q\bar{q} \text{ from jet ladder} \otimes t \otimes \Psi_1 \Psi_2). \quad (85)$$

This expression differs from (81) by the initial state only, which is the wave function of $q\bar{q}$ -pair for a jet ladder but not for the state defined by the wave function Ψ_{in} . This means that the ratio of probabilities of producing a strange and a non-strange quark are given by the factor m^2/m_s^2 . So, one has the same $\lambda \simeq 0.5$ value as in the decay process, which does not contradict the experimental data on the ratio of yields K^\pm/π^\pm . The ratio K^\pm/π^\pm as a function of x is shown in Fig.16e. It is seen that at $x = 0.2$ $K^\pm/\pi^\pm \simeq 0.35$. With the increase of x the ratio K^\pm/π^\pm grows and reaches the value ~ 0.8 at $x = 0.7$. Such an increase is rather legible: indeed, K mesons are produced both due to the formation of a new $s\bar{s}$ pair in the ladder (with the probability λ) and to the fragmentation production of an $s\bar{s}$ pair in the transition $Z^0 \rightarrow s\bar{s}$. Relative probabilities of prompt production of $Z^0 \rightarrow u\bar{u}, d\bar{d}, s\bar{s}$ obey the ratio $u\bar{u} : d\bar{d} : s\bar{s} \simeq 0.26 : 0.37 : 0.37$. Because of that the production of K meson at large x is proportional to

$$K^+ \sim (0.37 \cdot 1 + 0.26 \cdot \lambda). \quad (86)$$

The same quantity for pions is

$$\pi^+ \sim (0.37 \cdot 1 + 0.26 \cdot 1). \quad (87)$$

So, the ratio K^+/π^+ at large x is equal to

$$\frac{K^+}{\pi^+} = \frac{0.37 + 0.26\lambda}{0.37 + 0.26} \simeq 0.8 \quad (88)$$

at $\lambda = 0.5$. This value agrees with the experimental data as it is demonstrated by Fig.16e, where $\lambda(x)$ determined as the $K^\pm/\pi^\pm(x)$ -ratio is shown.

The small value of K^+/π^+ at $x = 0$ is a direct consequence of large probability to produce highly excited resonances: in the resonance decay more pions than kaons are produced. For the problem of breeding of strange and non-strange states in the decay, it is rather interesting to see the ratio K^*/ρ — experimental data for K^{0*}/ρ^0 are shown in Fig.16e too (shaded area). Remarkably, the ratio K^{0*}/ρ^0 has no tendency to decrease with decreasing x : this means that the rate of breeding of K^{0*} and ρ^0 in decays is approximately the same. Unfortunately, experimental errors are too large to have more definite conclusions about the behaviour of $\lambda(x)$.

The suppression parameter for the production of a strange quark cannot be reliably determined. This is because the masses of strange and non-strange quarks are small compared to the mean transverse momenta of quarks in the production process, see (84). We can draw a more definite conclusion about the suppression parameter λ_Q for the production of heavy quarks $Q = c, b$. This parameter is defined by the same formula (79) for multiperipheral production, so we have:

$$\lambda_Q \simeq \frac{m^2}{m_Q^2 \ln^2 \frac{\Lambda^2}{m_Q^2}}. \quad (89)$$

Here we take into account that the gluon–quark coupling constant decreases with the growth of the quark mass, $\lambda_Q \sim \alpha^2(m_Q^2)$. The QCD scale constant, Λ , is of the order of 200 MeV.

To estimate λ_c and λ_b , let us use $m = 0.35$ GeV, $m_c = M_{J/\Psi}/2 = 1.55$ GeV, $m_b = M_{\Upsilon}/2 = 4.73$ GeV and $\Lambda = 0.2$ GeV. Then

$$\lambda_c \simeq 2.8 \times 10^{-3}, \quad \lambda_b \simeq 1.1 \times 10^{-4}. \quad (90)$$

The value of λ_c should reveal itself in the inclusive production of J/Ψ and χ mesons, while λ_b is to be seen in reactions with Υ 's: $Z^0 \rightarrow (\sum J/\Psi + \sum \chi) + X$ and $Z^0 \rightarrow \sum \Upsilon + X$. These reactions are determined by the processes $Z^0 \rightarrow c\bar{c} \rightarrow c + (\bar{c}c + \bar{q}q\text{-sea}) + \bar{c}$ and $Z^0 \rightarrow b\bar{b} \rightarrow b + (\bar{b}b + \bar{q}q\text{-sea}) + \bar{b}$: for the production of a $c\bar{c}$ or $b\bar{b}$ meson a new pair of heavy quarks should be produced, since the quarks formed at the first stage of the decay, $Z^0 \rightarrow c\bar{c}$ or $Z^0 \rightarrow b\bar{b}$, have a rather big gap in the rapidity scale. So, within the definition

$$\begin{aligned} \lambda_c &\simeq \Gamma\left(c\bar{c} \rightarrow c + (\bar{c}c + \bar{q}q\text{-sea}) + \bar{c}\right) / \Gamma(c\bar{c}) \\ \lambda_b &\simeq \Gamma\left(b\bar{b} \rightarrow b + (\bar{b}b + \bar{q}q\text{-sea}) + \bar{b}\right) / \Gamma(b\bar{b}), \end{aligned} \quad (91)$$

we estimate $\Gamma(c\bar{c} \rightarrow c + (\bar{c}c + \bar{q}q\text{-sea}) + \bar{c})$ and $\Gamma(b\bar{b} \rightarrow b + (\bar{b}b + \bar{q}q\text{-sea}) + \bar{b})$ by the available data from [49]. Roughly, we get

$$\lambda_c = (2.07 \pm 0.23) \times 10^{-3}, \quad \lambda_b = (0.31 \pm 0.19) \times 10^{-4}, \quad (92)$$

in a reasonable agreement with (90).

3.4 Baryon-meson ratio and the Watson-Migdal factor

Our present understanding of the multiperipheral ladder is not sufficient to re-analyse (9) on the level carried out in Sections 3.1 and 3.2 for V/P . Nevertheless, the data for decays $Z^0 \rightarrow p + X$ and $Z^0 \rightarrow \pi^+ + X$ definitely confirm the equation. Quark combinatorics [9] predicts for p/π^+ at large x :

$$p/\pi^+ \simeq 0.20 \quad (93)$$

In Fig.16d one can see the p/π^+ ratio given by the fit to the data [29] (shaded area) and the prediction of quark combinatorics (93): the agreement at $x > 0.2$ is quite good.

Let us comment the result of our calculation $p/\pi^+ \simeq 0.20$ for leading particles in jets. In the jet created by a quark the leading hadrons are produced in proportions as it is given by Eq.(7): $B_i : 2M_i : M$. We consider only the production of hadrons belonging to the lowest (baryon and meson) multiplets, and, hence, keep in (29), (30) only the terms with $L = 0$ (hadrons from the quark S -wave multiplets). In our estimations we assume $\beta_0 \simeq \mu_0$, and therefore we substitute $B_i \rightarrow B_i(0)$, $M_i \rightarrow M_i(0)$ and $M \rightarrow M(0)$. The precise content of $B_i(0)$, $M_i(0)$ and $M(0)$ depends on the proportions in which the sea quarks are produced. We assume flavour symmetry breaking for sea quarks (see (27)). For the sake of simplicity, we put first $\lambda = 0$ (actually the ratio p/π depends weakly on λ). Then for the u -quark initiated jet we have:

$$\begin{aligned} B_u(0) &\rightarrow \frac{2}{15}p + \frac{1}{15}n + (\Delta - \text{resonances}), \\ M_u(0) &\rightarrow \frac{1}{8}\pi^+ + \frac{1}{16}\pi^0 + \frac{1}{16}(\eta + \eta') + (\text{vector mesons}), \\ M(0) &\rightarrow \frac{1}{16}\pi^+ + \frac{1}{16}\pi^0 + \frac{1}{16}\pi^- + \frac{1}{16}(\eta + \eta') + (\text{vector mesons}). \end{aligned} \quad (94)$$

The hadron content of the d -quark initiated jet is determined by isotopic conjugation $p \rightarrow n$, $n \rightarrow p$, $\pi^+ \rightarrow \pi^-$, and the content of antiquark jets is governed by charge conjugation; in jets of strange quarks only sea mesons (M) contribute to the p/π^+ ratio.

Taking into account the ratio $B_i : 2M_i : M = 1 : 2 : 1$ and the probabilities for the production of quarks of different flavours q_i , given by (1), we obtain $p/\pi^+ \simeq 0.21$ for $\lambda = 0$. We can easily get the p/π^+ ratio for an arbitrary λ : the decomposition of the ensembles $B_i(0)$, $M_i(0)$, $M(0)$ with respect to hadron states has been performed in [9] (see Appendix D, Tables D.1 and D.2). But, as was stressed above, this ratio is a weakly dependent function of λ : at $\lambda = 1$ we have $p/\pi^+ \simeq 0.20$.

For quark combinatorics the saturation of $q\bar{q}$ and qqq states by real hadrons is of principal importance. The probability of saturation is defined by the coefficients $(\mu_L, \mu_L^{(i)})$ and $(\beta_L, \beta_L^{(i)})$ in (29,30). The main question is what contributions from higher multiplets are not negligible in the spectra.

Consider in more detail the production of mesons in the central region: $q\bar{q} \rightarrow M$. The central production of $q\bar{q}$ states is provided by the diagrams of Fig.18 (loop diagram, Fig.18a, and interactions of the produced quarks, Fig.18b). The diagrams of the type of Fig.18b for final state interactions lead to the relativistic Watson-Migdal factor. To estimate how many highly excited states are produced, we have to find out which states are determined by the $q\bar{q}$ system in the multiperipheral ladder.

The constructive element of the ladder is a process shown in Fig. 17b. In this process,

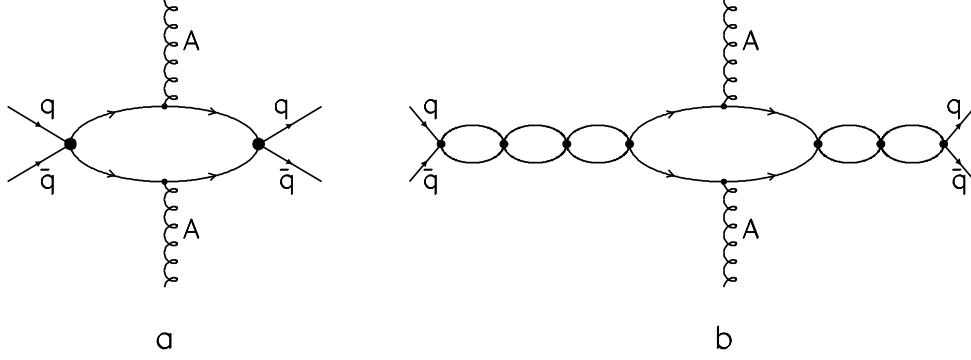


Fig.18

as was stressed in Section 3.3, new $q\bar{q}$ pairs are created at relatively large separations (in hadronic scale), at $r \sim 1$ fm: these separations are just those in the $q\bar{q} \rightarrow M$ transitions. The orbital momenta of the $q\bar{q}$ system for this transition can be written as $L \sim kr$. For relative quark momenta $k \leq 0.6$ GeV/c, we have

$$L \leq 3. \quad (95)$$

Relying on the behaviour of the Regge trajectory, one can understand, to what meson masses μ this relation corresponds. The trajectories for $q\bar{q}$ states are linear up to $\mu \sim 2.5$ GeV [73]:

$$\alpha(\mu^2) \simeq \alpha(0) + \alpha'(0)\mu^2, \quad (96)$$

the slope $\alpha'(0)$ is approximately equal $\alpha'(0) \simeq 0.8$ GeV⁻² and the intercept belongs to the interval $0.25 \leq \alpha(0) \leq 0.5$. Hence, for large μ , the estimation gives $\mu^2 \sim \alpha(\mu^2)/\alpha'(0)$; with $\alpha(\mu^2) \sim 3$, we have $\mu^2 \sim 4$ GeV². So we conclude that in the multiperipheral ladder it would be natural to expect the production of $q\bar{q}$ mesons with masses

$$\mu \leq 2 \text{ GeV}. \quad (97)$$

4 Hadron - nucleus interaction

We have demonstrated that the investigation of multiparticle production processes provides a good possibility to prove the main assumptions of the presented approach. There exist, however, processes, which allow us to observe the consequences of the spectator mechanism in a relatively pure way, i.e. we can prove the hypothesis which is crucial from the point of view of the hadron structure. These processes are the hadron - nucleus collisions at high energies. They enable us to test the hadron structure because of the well-known fact that at sufficiently high energies the specific picture of the beam fragmentation is not distorted by possible repeated collisions with the nuclear matter. (For details, see [9]). As we have discussed it already, due to the parton hypothesis secondaries need time to be formed ([19], [45]), which is proportional to their momenta p : $\tau \sim \frac{p}{m^2}$. Hence, the constituents go through the nucleus before forming a secondary hadron, and repeated interactions with the nucleus become impossible.

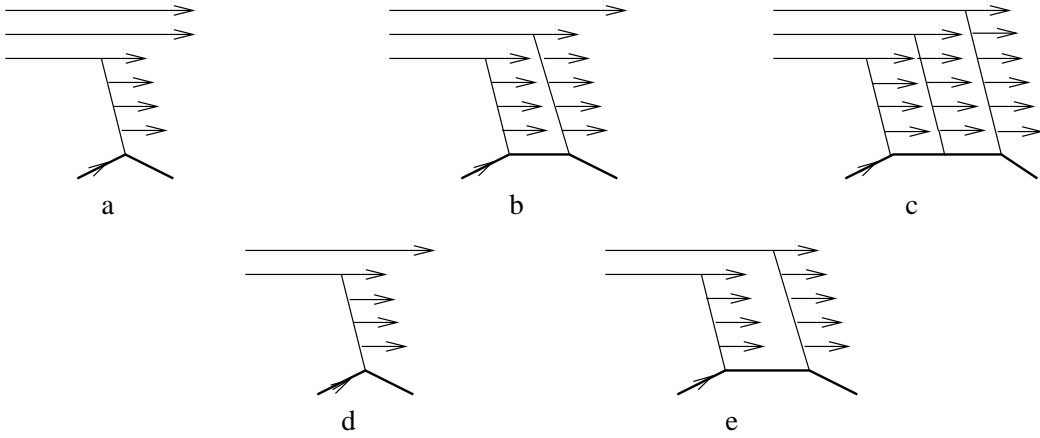


Fig.19

In hadron - hadron collisions only one pair of quarks takes part: one of the incident particle and one of the target. When, however, a hadron collides with a heavy nucleus, while going through the nuclear matter, its constituents can interact independently of each other with different nucleons of the nucleus. In the case of a superheavy nucleus all the constituents of the projectile would interact so that all three (or two) quarks of an incident baryon (or meson, respectively) would break up. (This would mean, e.g., that the multiplicity ratio of the secondaries for πA and pA interactions in the central region were $\sim 2/3$ [37]). For real nuclei (even for $A \sim 200$) a part of the constituent quarks still goes through a nucleus without interacting. The number of quarks passing the nucleus without interaction determines the multiplicity of the fragmentational hadrons, i.e. hadrons in the region of large x values.

Hence, in baryon - nucleus collisions three different processes are possible: one quark is interacting, two go through the nucleus (Fig.19a); two quarks are interacting and one goes through the nucleus (Fig.19b) and finally, all three quarks interact (Fig.19c). In meson - nucleus interactions one (Fig.19d) or two quarks (Fig.19e) of the incident meson can take part in the interaction.

The probability for a quark to interact can be calculated as a function of the distribution of the nuclear matter density and the inelastic quark - nucleon cross section:

$$\sigma_q \equiv \sigma_{inel}^{qN} \approx \frac{1}{3} \sigma_{inel}^{NN} \approx \frac{1}{2} \sigma_{inel}^{\pi N} \approx 10 \text{mbarn}.$$

The probabilities of these processes can be written as

$$V_k^h = \frac{n!}{(n-k)!k!\sigma_{prod}^{hA}} \int d^2b e^{-(n-k)\sigma_q T(b)} [1 - e^{-\sigma_q T(b)}]^k, \quad (98)$$

where k is the number of the interacting quarks, and h is the incident hadron consisting of n quarks ($n = 2$ for mesons and $n = 3$ for baryons ([20],[21])). The function $T(b)$ is expressed in terms of the nucleon distribution density in the nucleus:

$$T(b) = A \int_{-\infty}^{\infty} dz \rho(b, z). \quad (99)$$

For $\rho(r = \sqrt{b^2 + z^2})$, the Fermi parametrization,

$$\rho(r) = \frac{1}{1 + e^{[(r-c_1)/c_2]}}, \quad 4\pi \int_0^\infty \rho(r)r^2 dr = 1 \quad (100)$$

is accepted. The parameters c_1 and c_2 are taken from the data on eA scattering ([38],[39]). The probabilities σ_{prod}^{hA} for the hadron - nucleus scatterings have the same meaning as the inelastic hadron - hadron cross section with the production of at least one secondary hadron. It is obtained from the normalization condition $\sum_i V_i^h(A) = 1$:

$$\sigma_{prod}^{hA} \int d^2b [1 - e^{-n_q T(b)}]. \quad (101)$$

The values of the probabilities $V_i^h(A)$ which are calculated from the nuclear density functions found in eA scatterings for p , π and K beams (see [38]), are given in [22],[40]. For light nuclei processes with the interaction of only one constituent quark are dominating (Figs.19a, 19d). However, even for the nucleus of Be the share of the process with two interacting constituent quarks (Fig.19b) is not small (around 25%). For nuclei $A \sim 100$ the probabilities of all three processes of proton fragmentation are of the same order.

The calculation of the probability $V_i^h(A)$ allows us to obtain the relation between multiplicities in different regions of hadron - nucleus collisions.

We assume that the interacting dressed quarks produce secondary particles independently of each other. Then in the central region the multiplicities for the processes shown in Figs.19b, 19e is twice as large as in the processes Figs.19a, 19c; the ratio of the multiplicities for processes with three and one interacting quarks is three. Indeed, using (98), we can express the multiplicities $\langle n \rangle_{pA}$ and $\langle n \rangle_{\pi A}$ in the form

$$\begin{aligned} R\left(\frac{pA}{qA}\right) &= \frac{\langle n \rangle_{pA}}{\langle n \rangle_{qA}} = \sum_{k=1}^3 k V_k^p = \frac{3}{\sigma_{prod}^{pA}} \int d^2b [1 - e^{-\sigma(qN)T(b)}] \\ R\left(\frac{\pi A}{qA}\right) &= \frac{\langle n \rangle_{\pi A}}{\langle n \rangle_{qA}} = \sum_{k=1}^2 k V_k^\pi = \frac{2}{\sigma_{prod}^{\pi A}} \int d^2b [1 - e^{-\sigma(qN)T(b)}]. \end{aligned} \quad (102)$$

The ratio of multiplicities of the secondary particles in pA and πA does not depend on $\langle n \rangle_{qA}$ and is

$$R\left(\frac{pA}{\pi A}\right) = \frac{\langle n \rangle_{pA}}{\langle n \rangle_{\pi A}} = \frac{V_1^p(A) + 2V_2^p(A) + 3V_3^p(A)}{V_1^\pi(A) + 2V_2^\pi(A)} = \frac{3 \sigma_{prod}^{\pi A}}{2 \sigma_{prod}^{pA}}. \quad (103)$$

For heavy nuclei $\sigma_{prod}^{\pi A}/\sigma_{prod}^{pA} \approx 1$, and we obtain relation (4). The comparison of $R(pA/\pi A)$ with the experimental data [22] is presented in Fig.20.

The calculated value of $R\left(\frac{pA}{\pi A}\right)$ is in agreement with experiment in the interval $1, 5 < \eta < 3, 5$ for the nuclei C($A=12$) and Pb($A=207$) and for photoemulsion $1/2 \text{ Ag} + 1/2 \text{ Br}$. The considered region for the values of the quasirapidity $\eta = -\ln \tan \theta/2$ corresponds just to the central region of the collision processes.

Due to (102), the ratios of the secondaries in πA and πp scatterings and in pA and pp scatterings depend on the ratios $\langle n \rangle_{qA} / \langle n \rangle_{qq}$ (where $\langle n \rangle_{qq}$ is the multiplicity in the quark-quark collision):

$$R\left(\frac{\pi A}{\pi p}\right) = [V_1^\pi(A) + 2V_2^\pi(A)] \frac{\langle n \rangle_{qA}}{\langle n \rangle_{qN}}, \quad (104)$$

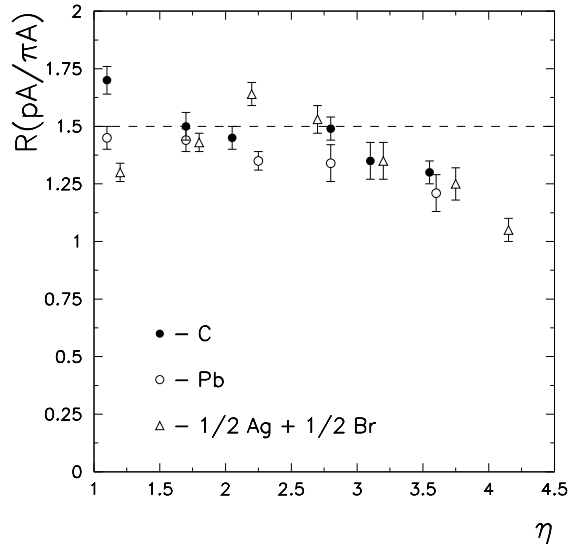


Fig.20

$$R\left(\frac{pA}{pp}\right) = [V_1^p(A) + 2V_2^p(A) + 3V_3^p(A)] \frac{\langle n \rangle_{qA}}{\langle n \rangle_{qN}}. \quad (105)$$

The relation (103) is reasonably well satisfied experimentally, and we can take $\langle n \rangle_{qA} \simeq \langle n \rangle_{qN}$.

Further, the multiplicities of secondary hadrons in the fragmentation region are calculated as functions of the atomic number A of the target. The values of $V_1^p(A)$, $V_2^p(A)$, $V_3^p(A)$ and σ_{prod}^{pA} are shown in Fig.21. The proton-nucleus cross section increases as $A^{2/3}$, in full accordance with expectations.

As already said, the model with three spatially separated quarks enables us to express the multiplicity of a fast secondary baryon with $x \simeq 2/3$ for proton - nucleus collisions in terms of the multiplicity for pp interactions. In both cases a fast baryon is produced by picking up a newly made quark of the sea by the two non-interacting spectators. The upper vertices in Figs.9b and 19a coincide, so they cancel in the ratio of the cross sections or multiplicities. Therefore the ratio of the inclusive cross sections must not depend on x in a region near $x = 2/3$. This independence on x provides a test of the hypothesis that the three constituents in a nucleon are spatially separated, whatever the formation mechanism of the secondaries is.

The calculated ratio of the absolute proton yields with nucleus and proton targets is

$$\frac{\frac{d^2\sigma}{dpd\Omega}(pA \rightarrow pX)}{\frac{d^2\sigma}{dpd\Omega}(pp \rightarrow pX)} = V_1^p(A) \frac{\sigma_{prod}^{pA}}{\sigma_{inel}^{pp}} \quad (106)$$

at $x \simeq 2/3$. The results of our calculations are displayed in Fig.22a for the nuclei of Be, Al, Cu and Pb together with data obtained at 19, 2 GeV/c [39]. Theory and experiment are consistent in the wide range $0,55 \leq x \leq 0,85$ where the experimental x -dependence of the ratio (106) is essentially flat. This indicates the absence of a substantial spread in momenta of the constituents.

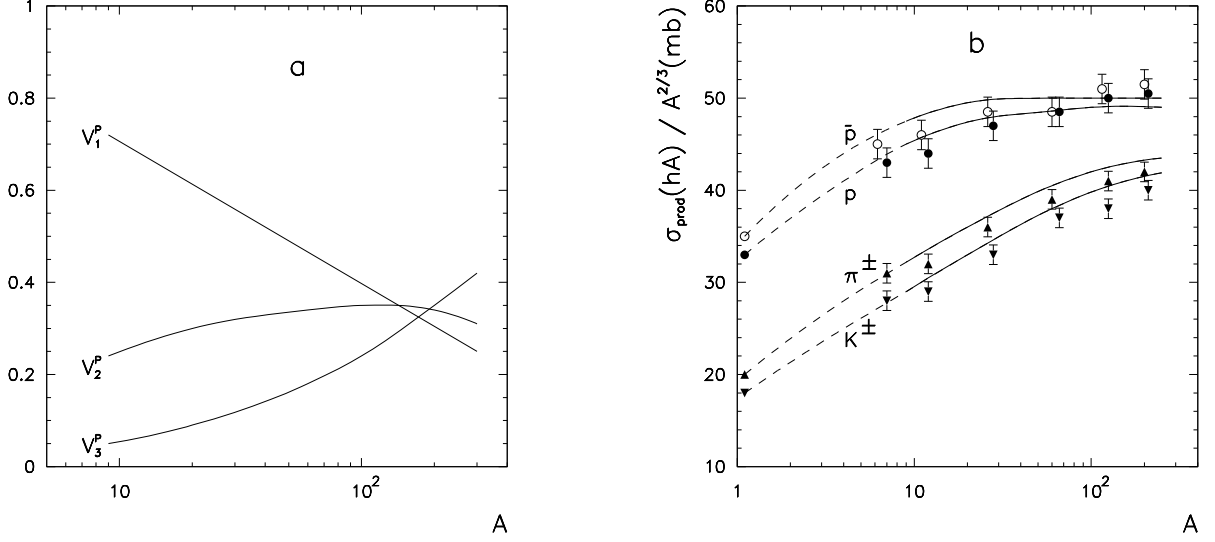


Fig.21

The experimental values of V_1^p obtained from the data of [40] are shown in Fig.22b to be consistent with our calculation.

The ratio of the meson yields near $x = 1/3$ is obtained by using the expressions (7), (8):

$$\frac{\frac{1}{\sigma_{prod}^{pA}} \frac{d^2\sigma}{dpd\Omega}(pA \rightarrow MX)}{\frac{1}{\sigma_{inel}^{pp}} \frac{d^2\sigma}{dpd\Omega}(pp \rightarrow MX)} = V_1^p(A) + \frac{4}{5}V_2^p(A). \quad (107)$$

In Fig.23 we plot the values of $V_1^p + 4/5V_2^p$ calculated according to Eq.(98). Also shown are the experimental values of the left-hand side of (107), obtained from the data of [40] on π^- and k^+ yields at $p_{lab} = 19, 2GeV/c$, $\theta = 12, 5mrad$ and $x = 0, 34$ for Be, Al, Cu and Pb nuclei. Agreement between theory and experiment is quite good. The π^- and K^+ mesons have been chosen, since the chance of producing such particles near $x = 1/3$ as resonance decay products is negligible. The opposite case of π^+ production at $x \simeq 1/3$ is probably dominated just by the baryonic resonance decays, and therefore we do not consider them here.

When a pion strikes a nucleus or a proton, the ratio of inclusive spectra of the same fragments at $x \simeq 1/2$ containing one of the pion quarks must be

$$\frac{\frac{1}{\sigma_{prod}^{\pi A}} \frac{d^2\sigma}{dpd\Omega}(\pi^- A \rightarrow hX)}{\frac{1}{\sigma_{inel}^{\pi p}} \frac{d^2\sigma}{dpd\Omega}(\pi^- p \rightarrow hX)} \quad h = \pi^-, \pi^0, p, n, \dots$$

independently of the kind of the secondary particle. Hence, the single-hadron yield ratios like π^-/K^- , π^-/p etc., must be the same (at $x \simeq 1/2$) for all nuclei in $\pi^- A$ interactions. The theoretical A dependence of V_1^π shown in Fig.22b can be given as

$$V_1^\pi(A) \simeq 1,75A^{-0,24}$$

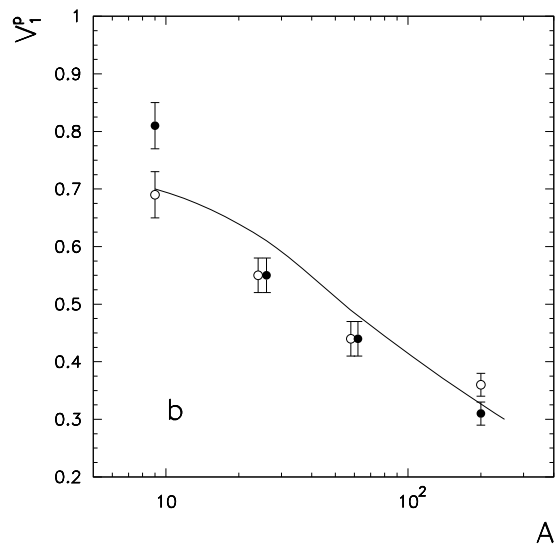
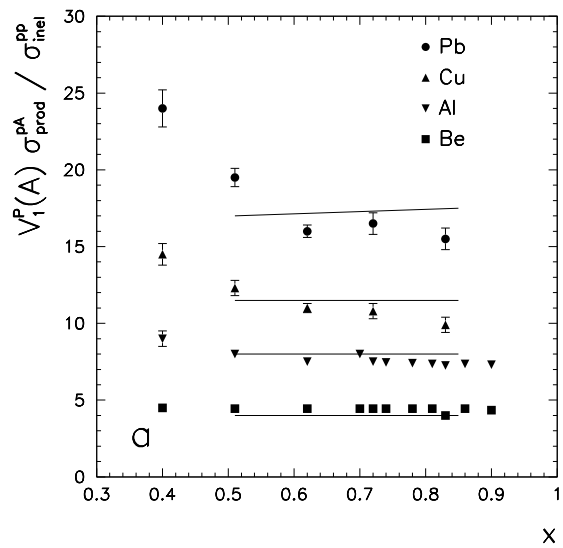


Fig.22

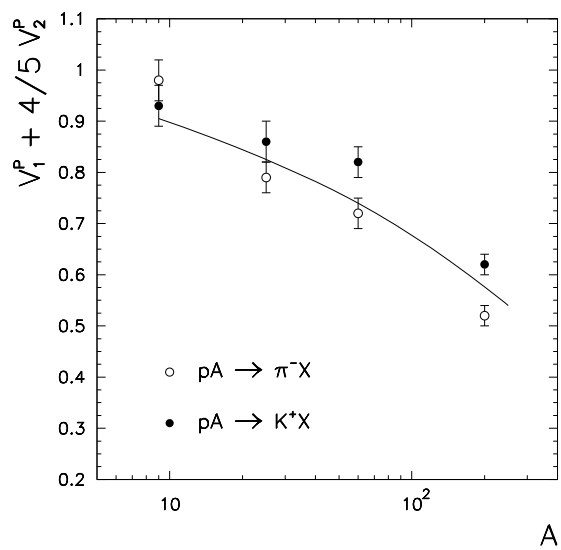


Fig.23

for $A > 60$.

If the incident particle is a kaon, the production of a fragment containing the strange quark is determined by the probability to absorb the non-strange quark, V_q^k . For instance, for the K^- beam the spectra of strange secondaries K^- , \bar{K}^0 , Λ , Σ etc. must be in the ratio

$$\frac{\frac{1}{\sigma_{prod}^{KA}} \frac{d^2\sigma}{dpd\Omega}(K^- A \rightarrow h_s X)}{\frac{1}{\sigma_{inel}^{Kp}} \frac{d^2\sigma}{dpd\Omega}(K^- p \rightarrow h_s X)} = V_q^K(A) \left(1 + \frac{\sigma_s}{\sigma_q}\right), \quad h_s = K^-, \Lambda, \Sigma, \dots$$

According to Fig.22b, $V_q^K(A) \simeq 0,82A^{-0,15}$ for $A > 30$. On the other hand, the ratio of the spectra of non-strange fragments like π^0 , π^- , \bar{N} etc. is determined by the probability to absorb the strange quark:

$$\frac{\frac{1}{\sigma_{prod}^{KA}} \frac{d^2\sigma}{dpd\Omega}(K^- A \rightarrow hX)}{\frac{1}{\sigma_{inel}^{Kp}} \frac{d^2\sigma}{dpd\Omega}(K^- p \rightarrow h_s X)} = V_s^K(A) \left(1 + \frac{\sigma_s}{\sigma_q}\right), \quad h = \pi^-, \pi^0, \bar{p}, \bar{n} \dots$$

In the case of a hyperon beam (Λ or Σ) near $x = 2/3$ the multiplicity ratio for the baryons, containing the strange quark, is again determined by the probability of absorbing a non-strange quark, say $V_{1q}^\Lambda(A)$. On the other hand, a similar ratio for the non-strange baryons. As can be seen, the difference in the A dependences of these quantities is very small. Experimental observation of the predicted decrease of the multiplicity ratio for strange and non-strange hadrons near $x = 1/2$ in the case of a kaon beam would be a verification of the hypothesis of the small cross section for a strange quark interacting with a nucleon.

Similarly to the hadron-hadron interactions, in the hadron-nucleus interaction processes we can observe the production of fast secondary hadrons. Due to the presented mechanism of the interaction, we have to consider those cases, when one or two constituents of the incident baryon ($x \sim 2/3$ and $x \sim 1/3$, respectively) and one constituent of the incident meson ($x \sim 1/2$) participate in the interaction. Using the expressions (7) and (8), we have for the baryon-nucleus collision

$$\begin{aligned} & V_1^b(A)(q_i q_j + q, \bar{q} - sea) + V_2^b(A)(q_i + q, \bar{q} - sea) \\ & \rightarrow V_1^b \left(\frac{1}{2} B_{ij} + \frac{1}{12} (B_i + B_j) + \frac{5}{12} (M_i + M_j) \right) \\ & + V_2^b \left(\frac{1}{3} B_i + \frac{2}{3} M_i \right). \end{aligned} \quad (108)$$

In addition, the following distribution functions have to be introduced: $f_{ij}(x, p_\perp^2)$ for B_{ij} , $f_i(x, p_\perp^2)$ for B_i and $\varphi_i(x, p_\perp^2)$ for M_i . We assume $f_{uu} = f_{ud} = f_{dd}$; $\varphi_u = \varphi_d$, $f_u = f_d$. Instead of (104) we then have

$$\begin{aligned} & V_1^b(A) \left[\frac{1}{2} f_{ij}(x) B_{ij} + \frac{1}{12} (f_i(x) B_i + f_j(x) B_j) + \frac{5}{12} (\varphi_i(x) M_i + \varphi_j(x) M_j) \right] \\ & + V_2^b(A) \left(\frac{1}{3} f_i(x) B_i + \frac{2}{3} \varphi_i(x) M_i \right). \end{aligned} \quad (109)$$

The meson-nucleus collision can be described as

$$V_1^m(A)(q_i + q, \bar{q} - sea) \rightarrow V_1^m(A) \left(\frac{1}{3} B_i + \frac{2}{3} M_i \right)$$

$$\rightarrow V_1^m(A) \left(\frac{1}{3} f_i(x) B_i + \frac{2}{3} \varphi_i(x) M_i \right). \quad (110)$$

Similarly to the hadron-hadron collisions case, one can easily get the secondary particles produced in pA , ΛA , ΣA , πA etc. processes.

Acknowledgements

The author would like to thank V.V. Anisovich and V.N. Nikonov for many helpful discussions during the preparation of this review.

References

- 1 M. Gell-Mann, Phys.Lett. **8** 214 (1964)
- 2 G. Zweig, CERN report 8419/TH 412 (1964)
- 3 G. Morpurgo, Physics **2** 95 (1965)
- 4 R.H. Dalitz, Proceedings of the Berkeley Conference (1966)
- 5 E.M. Levin, L.L. Frankfurt, JETP Pisma **3** 652 (1965)
- 6 H.J. Lipkin, F. Scheck, Phys. Rev. Lett. **16** 71 (1966)
- 7 J.J.J. Kokkedee, L. Van Hove, Nuovo Cim. **42** 711 (1966)
- 8 V.N. Gribov, Eur. Phys. J. **C10** 71 (1999), e-print Archive hep-ph/9807224; Eur. Phys. J. **C10** 91 (1999), e-print Archive hep-ph/9902279
- 9 V.V. Anisovich, M.N. Kobrinsky, J. Nyiri, Yu.M. Shabelski, World Scientific, Singapore (1985)
- 10 V.V. Anisovich, Proceedings of the 9th LNPI Winter School on Nuclear and Elementary Particle Physics, Leningrad (1974)
- 11 V.V. Anisovich, Proceedings of the 14th LNPI Winter School on Nuclear and Elementary Particle Physics, Leningrad (1979)
- 12 V.N. Gribov, autumn session of the Academy of Sciences USSR, Moscow (1977)
- 13 E.V. Shuryak, Phys.Rept. **115** 151 (1984)
- 14 E.M. Levin, M.G. Ryskin, Yad. Fiz. **21** 1072 (1975)
- 15 N. Cabibbo, R. Petronzio, CERN preprint TH 2440 (1978)
- 16 E.M. Levin, V.M. Shekhter, Proceedings of the 9th LNPI Winter School on Nuclear and Elementary Particle Physics, Leningrad (1974)
- 17 J.P. Burq et al., Nucl. Phys. B **217** 285 (1983)

- 18 S. Bondarenko, E. Levin, J. Nyiri, TAUP-2700-2002 (2002), e-print Archive hep-ph/0204156
- 19 V.N. Gribov, Proceedings of the 8th LNPI Winter School on Nuclear and Elementary Particle Physics, Leningrad (1973)
- 20 V.V. Anisovich, V.M. Shekhter, Nucl. Phys. **B55**, 455 (1973)
- 21 J.D. Bjorken, G.E. Farrar, Phys. Rev. **D9**, 1449 (1974)
- 22 V.V. Anisovich, F.G. Lepekhin, Yu.M. Shabelsky, Yad. Fiz. **27** 1639 (1978)
- 23 V.V. Anisovich, Yu.M. Shabelsky, V.M. Shekhter, Nucl. Phys. **B133** 477 (1978)
- 24 F.E. Close, Yu.L. Dokshitzer, V.N. Gribov, V.A. Khoze and
- 25 V.N. Gribov, Effective Theories and Fundamental Interactions, Proceedings of the International School of Subnuclear Physics, Erice **34**, 42 (1996)
- 26 V.V. Anisovich, Yad. Fiz. **28** 761 (1978)
- 27 V.V. Anisovich, M.N. Kobrinsky, J. Nyiri, LNPI preprint 631 (1980); Yad. Fiz. **34** 195 (1981) (Sov. J. Nucl. Phys. **34** 111 (1981))
- 28 V.V. Anisovich, J. Nyiri, Yad. Fiz. **30** 539 (1979) (Sov. J. Nucl. Phys. **30** 279 (1980))
- 29 ALEPH Collaboration, R. Barate et al., Phys. Rep. **294** 1 (1998)
- 30 K. Böckmann, Invited Talk at the Meeting on Multiparticle Production Processes and Inclusive Reactions at High Energies, Serpukhov (1976)
- 31 A. Białas, Invited Talk at the First Workshop on Ultra-Relativistic Nuclear Collisions, LBL (1979); Fermilab-Conf. 79/35-TH4 (1979)
- 32 V.A. Nikonov, J. Nyiri, e-print Archive hep-ph/0006219 ,
V.V. Anisovich, V.A. Nikonov, J. Nyiri, e-print Archive hep-ph/0008163; Phys. Atom. Nucl. **64** 812 (2001); Yad. Fiz. **64** 877 (2001)
- 33 S.S. Gershtein, A.K. Likhoded, Yu.D. Prokoshkin, Z. Phys. **C24**, 305 (1984)
- 34 C. Amsler, F.E. Close, Phys. Rev. **D53**295 (1996)
- 35 V.V. Anisovich, Phys. Lett. **B364** 195 (1995)
- 36 Yu.L. Dokshitzer, XIth Rencontres de Blois (1999)
- 37 H. Überall, Electron Scattering from Complex Nuclei, part A, New York – London (1971)
- 38 L. Elton, Nuclear sizes, Oxford (1961)
- 39 Yu.M. Shabelski, Yad. Fiz. **33** 1379 (1981)
- 40 J.V. Allaby et al., Preprint CERN 70-12 (1970)

- 41 H. Kichimi et al., Lett. Nuovo Cim., **24**, 129 (1979); Phys. Rev. **D20**, 37 (1979).
A. Suzuki et al., Lett. Nuovo Cim., **24**, 449 (1979)
- 42 C. Cochet et al., Nucl. Phys. **B155**, 333 (1979)
- 43 V.M. Shekhter and L.M. Shcheglova, Yad. Fiz. **27** 1070 (1978); Sov. J. Nucl. Phys. **27** 567 (1978)
- 44 V.V. Anisovich, M.N. Kobrinsky, J. Nyiri, Phys. Lett. **B102** 357 (1981)
- 45 M.A. Voloshin, Yu.P. Nikitin and P.I. Porfirov, Sov. J. Nucl. Phys. **35** 586 (1982)
- 46 Yi-Jin Pei, Z. Phys. **C72** 39 (1996)
- 47 P.V. Chliapnikov, CERN-EP/99-142 (1999); Phys. Lett. **B462** 341 (1999)
- 48 Particle Data Group, C. Caso et al., Eur. Phys. J. **C3** 1 (1998)
- 49 C.A. Baker, C.J. Batty, P. Blüm et al., Phys. Lett. **B449** 114 (1999)
- 50 A.V. Anisovich, C.A. Baker, C.J. Batty et al., Phys. Lett. **B452** 187 (1999); *ibid*, **B452** 173 (1999); *ibid*, **B452** 180 (1999); Nucl. Phys. **A651** 253 (1999)
- 51 A.V. Anisovich, V.V. Anisovich, Yu.D. Prokoshkin and A.V.Sarantsev, Z. Phys **A357** 123 (1997) ;
A.V. Anisovich, V.V. Anisovich and A.V.Sarantsev, Z. Phys **A359** 173 (1997); *ibid*,
Phys. Lett. **B395** 123 (1997)
- 52 V.V. Anisovich, D.V. Bugg and A.V.Sarantsev, Phys. Rev. **D58**: 111503 (1998)
- 53 L3 Collaboration, M. Acciari et al., Phys. Lett. **B393** 465 (1997); *ibid*, **B407** 389 (1997)
- 54 DELPHI Collaboration, P. Abreu et al., Phys. Lett. **B475** 429 (2000); *ibid*, **B449** 364 (1999)
- 55 OPAL Collaboration, K. Ackerstaff et al., Eur. Phys. J. **C4** 19 (1998); G. Alexander et al., Z. Phys. **C73** 569, 587 (1997)
- 56 E.A. Kuraev, L.N. Lipatov and V.S. Fadin, Sov. Phys. JETP **44** 443 (1976); Ya.Ya. Balitsky and L.N. Lipatov, Sov. J. Nucl. Phys. **28** 822 (1978)
- 57 L.N. Lipatov, Sov. Phys. JETP **63** 904 (1986)
- 58 V.V. Anisovich, D.I. Melikhov and V.A. Nikonov, Phys. Rev. **D52** 5295 (1995); **D55** 2918 (1997)
- 59 V.V. Anisovich, D.I. Melikhov, B.Ch. Metsch and H.R. Petry, Nucl. Phys. **A563** 549 (1993)
- 60 T. Barnes, in Hadron Spectroscopy, AIP Conference Proceedings, Woodbury, New York (1998)

- 61 V.V. Anisovich, M.G. Huber, M.N. Kobrinsky and B.Ch. Metsch, Phys. Rev. **D42** 3045 (1990); V.V. Anisovich and B.Ch. Metsch, Phys. Rev. **D46** 3195 (1992)
- 62 ALEPH Collaboration (D. Busculic et al.), Z. Phys. **C69** 393 (1996)
- 63 DELPHI Collaboration (P. Abreu et al.), Z. Phys. **C68** 353 (1995)
- 64 L3 Collaboration, M. Acciari et al., Phys. Lett. **B345** 353 (1995);
- 65 OPAL Collaboration, K. Ackerstaff et al., Z. Phys. **C74** 413 (1997)
- 66 ALEPH Collaboration (R. Barate et al.), Preprint CERN/EP/99-94
- 67 DELPHI Collaboration (P. Abreu et al.), Preprint CERN/EP/99-66
- 68 OPAL Collaboration, K. Ackerstaff et al., Eur. Phys. J. **C5** 1 (1998)
- 69 D.B. Leinweber et al., Phys. Rev. **D58** 031501 (1998)
- 70 K.M. Watson, Phys. Rev. **88** 1163 (1952); A.B. Migdal, ZETF **28** 10 (1955)
- 71 M.A. Voloshin, Yu.P. Nikitin and P.I. Porfirov, Sov. J. Nucl. Phys. **35** 586 (1982)
- 72 K. Peters and E. Klempt, Phys. Lett. **B352** 467 (1995)
- 73 A.V. Anisovich, V.V. Anisovich and A.V. Sarantsev, e-Print Archive hep-ph/0003113, Phys. Rev. **D62** 051502 (R)